National University of Science and Technology
BUCHAREST POLYTECHNIC
Biotechnical Systems Engineering Doctoral School
Field: Environmental Engineering

THESIS
-SUMMARY-

PHOTOCATALYTIC NANOSTRUCTURED MATERIALS USED IN WASTEWATER DECONTAMINATION

SCIENTIFIC COORDINATOR,
Prof. univ. dr. habil. chem. Ecaterina MATEI

PhD student,
Eng. Alexandra Corina CONSTANDACHE

Bucharest
2023

CONTENT

INTRODUCTION

In recent years, the phenomenon of the spread of micropollutants in aquatic ecosystems has evolved into a global problem, which has led to an intensification of concerns regarding the integrity and health of the environment. Micropollutants represent a diversity of substances, both anthropogenic and natural, spanning categories such as pharmaceuticals, personal care products, steroid hormones, industrial chemicals, pesticides, and numerous other emerging compounds. Their wide variation and diversity creates difficulties in wastewater treatment processes.

Photocatalysis mediated by a semiconductor (typically a nanomaterial) is a well-established method for pollutant decomposition and the production of hydrogen through the decomposition of water, an environmentally friendly fuel.

Nanoparticles (NPs) have been integrated into the health, food, feed, space, chemical and cosmetic industries, which requires an environmentally friendly approach to their synthesis. Green chemistry has paved the way for the development of environmentally friendly approaches to nanoparticle synthesis. Different types of plants, bio-renewable materials or biological components, such as microorganisms, can thus be used. Plant extracts contain specific phytochemicals that simultaneously perform the roles of a reducing agent and a coating or stabilizing agent. ZnO NPs synthesized by green methods are non-toxic and biocompatible.

Considering these premises, the research carried out in the doctoral thesis aimed to investigate the photocatalytic characteristics of some nanocomposites for the elimination of a large number of pharmaceutical products from waste water.

Starting from previous research in the field of environmental and materials engineering, specific work protocols were made to obtain ZnO with photocatalytic characteristics, easy to recover from the environment, but also biocompatible at the same time.

The thesis includes 2 parts, the first part including an extensive study of the specialized literature, contained in 2 chapters that refer to the current state of research in the field of advanced materials with photocatalytic properties, used in environmental protection applications and respectively to the impact of emerging pollutants on the quality the aquatic environment. Based on these relevant data from the literature, the second part of the thesis was made, which includes the experimental researches, structured in 4 chapters that include the research methodology and plan, the methods of synthesis and characterization of the obtained materials and the results of the photocatalytic degradation tests.

The thesis also includes a chapter of general conclusions, personal contributions and future research directions.

CHAPTER I. THE CURRENT STAGE OF RESEARCH IN THE FIELD OF ADVANCED MATERIALS WITH PHOTOCATALYTIC PROPERTIES USED IN ENVIRONMENTAL PROTECTION APPLICATIONS

I.1. The importance of nanotechnologies in industrial and environmental applications

Nanotechnology has made enormous progress in recent decades with a 25-fold increase in the number of products that either contain or require nanoparticles (NPs) for their production between 2010 and 2020 [1]. This development is likely facilitated by their unique overall properties (particularly particle size, distribution, morphology, surface area, and shape) relative to their bulk or dissolved counterparts. This enables a wide range of possible applications, including their use in fields such as cosmetics, medicine, biology and catalysis.

As the world faces drinking water shortage, scientists have proven that nanomaterials are a superior option for wastewater treatment due to the fact that they have certain exclusive characteristics such as large surface area, nanometric size, highly reactive, mechanical stability good and good mobility in solution. Numerous studies have shown that nanomaterials can effectively remove various pollutants from water and thus have been successfully applied in wastewater treatment. For example, heavy metals (such as Pb, Mo, etc.) , organic pollutants, inorganic anions, and bacteria have been successfully removed from wastewater with the help of various nanomaterials.

I.2. Applications of nanomaterials in water decontamination

I.2.1. The impact of nanomaterials on the aquatic environment

In the past few years, the performance of nanomaterials has been explored in several aqueous environments, including oceans, rivers, lakes, and wetlands. A collective concern of research organizations has been to search for environmentally friendly remedial agents to launch a green economy for the purpose of soil and water decontamination. Currently, nanomaterials are generally used for wastewater treatment, and nano-photocatalytic technology is also commonly used to oxidize many organic compounds in water by producing hydroxide ions as well as strong oxidizing superoxide ions and higher activity. Nanomaterials exhibit different behaviors in aqueous environments, some having a positive and others a negative impact on biodiversity.

I.2.2. Photocatalysis – versatile technique applied for the degradation of organic pollutants

To date, photocatalysis has been considered one of the most attractive options for wastewater treatment due to its great potential and high efficiency by using sunlight to remove organic pollutants and harmful bacteria with the help of a photocatalyst.

Photocatalysis is a particular type of heterogeneous catalysis based on the use of a semiconductor (such as TiO_2 or ZnO) activated by light radiation (UV or visible). The concept of photocatalysis involves a combination of photochemical phenomena and catalysis processes. This means that both the presence of light and a catalyst are required to initiate or accelerate a chemical reaction. In short, photocatalysis can be defined as "acceleration of a photoreaction in the presence of a catalyst" [1].

In an ideal photocatalytic scenario, organic pollutants are converted into carbon dioxide (CO_2), water (H_2O) and mineral acids. This reaction takes place in the presence of metal oxide particles, such as TiO_2 or ZnO, and reactive oxidizing species, such as oxygen or air.

I.3. Photocatalytic materials applied in water decontamination processes

Nanotechnology is in continuous development being a new field of research dealing with the synthesis of nanoparticles (NPs) and nanomaterials for their applications in various fields such as electrochemistry, photocatalysis, sensors, biomedicine, pharmaceutical industry, health care, cosmetics, technology food, textile industry, mechanics, optics, electronics, space industry, energy science, optical devices, etc. Environmental decontamination by catalytic reduction of harmful organic contaminants has received increased attention in research nowadays [2]. Considering the catalytic application of nanomaterials in water treatment, nanomaterials can be classified into two types: carbon-based nanomaterials and metal and metal oxide-based nanomaterials.

Despite all the progress in the field, better knowledge is needed regarding the scale-up of photocatalytic reactors based on metal oxide nanoparticles. Various design aspects must be addressed before scaling up multiphase photocatalytic reactors. The uniform distribution and intensity of light inside the reactor are among the most important parameters, since the light penetration depth in the suspension containing the catalyst is about 2 cm. Moreover, a large surface area is required to cover the catalyst per unit volume of the reactor. This will require technical developments to translate experiments from laboratory scale to pilot scale and finally to large scale. In such reactors, solid catalyst installation, light loss

minimization, reactant-catalyst contact, flow pattern, mass transfer, mixing, reaction kinetics, and temperature must be considered [3].

I.4. ZnO – photocatalytic material with high performance in wastewater decontamination

ZnO has become a prime candidate for use as a catalyst in ecological management systems due to its unique characteristics. Among these features are a direct and wide band gap, especially in the near ultraviolet (UV) spectral region, strong oxidation capacity, excellent photocatalytic performance, and high exciton free binding energy. These properties allow excitonic emission processes to persist at ordinary or even higher temperatures. ZnO comes in the form of a white hexagonal crystal or a white powder called zinc white. Its crystal structure is wurtzite, similar to that of GaN, but in most cases, ZnO is found as a single crystal. It should also be noted that ZnO is odorless, has a bitter taste and dissolves in water. Due to its significant role as a semiconductor material, ZnO has found applications in areas such as catalysis, the rubber and paint industry, the production of ceramic objects, fertilizers and even in cosmetics.

In order to achieve a high yield of ZnO photocatalyst in the heterogeneous photocatalysis reaction, it is necessary to develop a suitable architecture that minimizes [4**Error! Bookmark not defined.**].

I.4.1. Synthesis methods of ZnO nanostructured materials

Zinc is a fairly active element and at the same time a strong reducing agent. Depending on its reduction potential it can be easily oxidized, forming zinc oxide, which is very useful in the preparation of zinc oxide nanoparticles [5].

There are two general strategies to approach the synthesis methods of zinc oxide nanomaterials: the "bottom-up" approach and the "top-down" approach. Thus, the "bottom-up" approach involves using atoms and molecules in a controlled manner to create nanostructures that can be obtained by chemical synthesis and biological methods. In contrast, the "top-down" approach involves reducing the dimensions of a larger material by fragmenting or grinding it to obtain nanometer-sized particles, these being the physical methods. Both strategies are used to prepare nanostructures on a large industrial scale.

It is important to note that each synthesis method has its own advantages and disadvantages, and the selection of the right method depends on the specific application and the properties desired in the final material. Also, combining different methods or approaches can lead to optimal properties in zinc oxide nanomaterials.

In addition to knowing the synthesis methods, an important problem as well as a challenge is finding a way to control the shape and size of the nanostructures. These parameters influence the optical properties of the nanoparticles, therefore it is important to select the most suitable synthesis method. In addition, it should be possible to choose the simplest, most efficient and, since the demand is increasing, the most environmentally friendly method (so-called green chemical synthesis) [6].

I.4.2. Properties of NP-ZnO using biosynthesis

Obtaining nanoparticles using living organisms is a promising method for the development of new materials that are safe, stable, economically convenient, and environmentally friendly with the help of the ecological approach in chemistry. However, the green synthesis of nanoparticles can also enhance the properties of these nanomaterials due to the reduced size and shape obtained and the specific properties of the biological substrates used .

In the case of NP-ZnO, green synthesis has been shown to improve properties such as antimicrobial activity, photocatalytic efficacy and biocompatibility. Therefore, ZnO NPs synthesized by the green method have a great potential to replace conventional ZnO NPs and be applied in the development of nanocomposites. To summarize, biological methods for the synthesis of ZnO nanoparticles appear to be cheap, environmentally friendly and much safer than the chemical approach.

I.4.3. Applications of phytogenic NP-ZnO

The US Food and Drug Administration (FDA) has described ZnO as a "GRAS" (Generally Recognized As Safe) material [7]. ZnO in nano size is much more easily absorbed by the body than in any other form. NP-ZnO have applications in various fields of medicine, industry, food, agriculture and electronics. Therefore, viable and easy large-scale production of the material is of interest. Phytogenic ZnO NPs have been extensively studied for their biological applications and remediation of environmental problems [8].

I.5. Photocatalytic degradation performances using ZnO obtained by the green method

Among the metal oxide NPs, NP-ZnO obtained by the green method has been widely used as a semiconductor photocatalyst due to its high reaction rate, large number of available reactive sites, high hydrogen peroxide generation efficiency, low cost, and environmentally friendly nature [9**Error! Bookmark not defined.Error! Bookmark not defined.**]. It has been established that ZnO exhibits high efficiency in the photodegradation of pollutants and

can be used in large-scale wastewater treatment. Table 1.1. summarizes recent reports on phytogenic ZnO nanoparticles used for photodegradation.

Table 1. 1 Photocatalytic performance of phytogenic ZnO nanoparticles.

No. Crt.	The green source	Morphology	Size	Pollutant	Irradiation source	Ref.
1	*Garcinia mangostana* fruit extract	Spherical	21 nm	Malachite green	Sunlight	[10]
2	Fruit pulp of *Aegle marmelos*	Spherical	30 nm	Methyl blue	UV light	[11]
3	*Azadirachta indica* leaf extract	Spherical	9.6-25.5 nm	Methyl blue	UV light	[12]
4	*Dolichos lablab L* leaf extract.	Hexagonal and triangular	7-49 nm	Methyl Blue, Rhodamine B and Orange II	Visible and UV light	[13]
5	*Hibiscus rosasinensis* leaf extract	Spherical	15-170 nm	Palm oil factory effluent	UV light	[14]
6	*Scutellaria baicalensis* root extract	Spherical	50 nm	Methyl blue	UV light	[15]
7	*Sechium edule* leaf extract	Spherical	32.6 nm	Reagent blue 160	UV light	[16]
8	Leaf extract of *Vitex trifolia L.*	Variable	28 nm	Methyl blue	UV light	[17]
9	*Carissa edulis* extract	Flower shape	50-55 nm	Congo red	UV light	[18**Error! Bookmark not defined.**]
10	*Calotropis procera* leaf extract	Spherical	15-25 nm	Methyl orange	UV light	[19]
11	*Hippophae rhamnoides* leaf extract	Flower shape	20.17 nm	Eosin	UV light	[20]

Regarding the use of organic polymer-supported ZnO to degrade wastewater contaminants, studies using polypropylene, polystyrene, polyurethane, poly(methyl methacrylate) and alginate have been reported [21]. Regarding the use of alginate, it is commonly used as a thickening, stabilizing, film-forming, gel-making and emulsion-stabilizing agent.

The photocatalyst immobilized on a polymer has several advantages: (1) it is very durable and can be used for a long time; (2) it is cheap and easy to obtain; (3) because it is hydrophobic, organic contaminants are adsorbed on the surface, thus improving the photocatalytic performance; (4) can be transformed into a variety of forms that can be perfectly combined with the catalyst [9**Error! Bookmark not defined.**].

I.6. Environmental applications of sodium alginate-based biopolymers

I.6.1. General knowledge of sodium alginate

Alginate is the most abundant polysaccharide up to 40% of the dry weight and is commonly available in the cell wall of brown seaweeds. It can form a viscous gum with water and has the ability to absorb about 200-300 times its weight in water . Alginate is a hydrophilic colloidal carbohydrate extracted using a dilute alkaline solution, which allows the formation of an insoluble gel by calcium cation gelation . The thickening, gel-forming, and stabilizing properties of alginate make its widely used biopolymer a wider range of applications, including packaging, tissue engineering, drug delivery, and wound healing [22].

I.6.2. Composites based on sodium alginate used for dye removal

Alginate-based composites are manufactured as absorbents for both inorganic and organic contaminants. Adsorption mechanisms usually involve ion exchange and electrostatic interactions. The special functionalities of the encapsulated materials can bring other benefits depending on the needs and applications. Achieving environmental goals while supporting robust economic growth requires innovative wastewater treatment technologies.

The environmental applications of alginate depend in part on the fact that the surface-rich functional groups (e.g. carboxyl and hydroxyl) in alginate could capture metal or cationic ions through ion exchange between the cross-linking cations and target pollutants such as heavy metals or dyes .

First, alginate spheres can serve as a stable matrix for other types of absorbents that are much too fine in particle size and too difficult to separate from aqueous solution. These absorbents are usually carbon-based, such as AC, CNT, and GO. AC has been widely used for wastewater treatment. However, AC is mostly used as a fine powder, and the difficulty of separation and regeneration from the effluent can lead to significant loss of adsorbent [23].

In addition to activated carbon and graphene oxide, alginate has also been mixed with other engineered natural nanoparticles to form composites with improved adsorbing capabilities [24]. Also, titanium dioxide (TiO_2) immobilized in a calcium alginate sphere kept its photoactivity during all experiments, and the TiO_2-gel balls showed good stability in water to maintain their shape after several uses. .

Immobilization of microbial cells in alginate spheres has also received increasing interest for dye removal.

I.6.3. Other environmental applications

In addition to dyes, heavy metals, and antibiotics, alginate-based composites have also been used to remediate other pollutants. For example, MnO_2 -alginate composites and alginate-Fe_3O_4 composite have been used to remove Sr(II) from seawater [25]. Removal of rare earth elements and radionuclides from water has been reported using various alginate-

based composites. In addition to cation removal, alginate-based nanomaterial composites have also been studied for the removal of some anions from water. Electrochemically modified calcium alginate-biochar spheres have also been applied to remove phosphate [26**Error! Bookmark not defined.**]. With continuous research and development, alginate-based nanocomposites will be increasingly applied in various areas of environmental remediation in the future.

I.7. Partial conclusions

Zinc oxide (ZnO) is the predominant semiconductor used in photocatalysis processes. It stands out for its high activity in the degradation of pollutants and has several important advantages, such as its non-toxic character, stability, and low production costs. Water pollution by various organic compounds, including CECs, such as PCPs, EDCs, pharmaceuticals, and pesticides is one of the major concerns of the 21st century. Due to their stability and difficult degradation, these compounds have been declared as priority substances in water policies. The use of nanophotocatalysts encapsulated in various composites has great potential for water remediation due to their superior catalytic properties and easy recovery, thus enabling easy reuse of the photocatalyst.

CHAPTER II. CURRENT STATE OF RESEARCH ON THE IMPACT OF EMERGING POLLUTANTS ON WATER QUALITY

II.1. Current knowledge on the occurrence of emerging contaminants in wastewater and surface water

In surface waters, a wide range of organic and inorganic contaminants are controlled by legislation presented by the European Commission [27]. These have traditionally been industrial or agricultural chemicals. However, the legislation is expected to expand to include a larger number of derived chemicals called CEs (emerging contaminants) following the recent proposal of pharmaceuticals as Priority Hazardous Substances.

CE are microorganisms and natural or synthetic chemicals not routinely regulated and/or monitored in the environment that have reached waterways and generally the hydrosphere with possible adverse effects on wildlife and human health (of example: personal care products, pesticides, heavy metals, surfactants, pharmaceuticals, solvents, etc.) [28**Error! Bookmark not defined.**].

Various techniques have been applied to degrade these organic contaminants, and advanced heterogeneous photocatalysis, involving the use of a zinc oxide (ZnO) photocatalyst, appears to be one of the most promising technologies in this regard. In recent years, the ZnO photocatalyst has been the subject of considerable interest due to its

outstanding characteristics. To achieve high yield in heterogeneous photocatalysis reactions, a suitable architecture is required to minimize electron loss during the excitation step and maximize photon absorption. To further improve the photo-induced charge carrier migration during the excitation stage, considerable effort is required to continue the development of heterogeneous photocatalysis under UV/visible/solar illumination [29].

II.2. Toxicological impact of emerging contaminants on the environment

Emerging contaminants can cause different toxicological responses between different species, depending on the concentration of the pollutant and the type of species studied.

Despite this, the data collected can give an indication of toxicity for most of the emerging contaminants. Non-steroidal anti-inflammatory drugs (acetaminophen, ibuprofen, diclofenac and naproxen), lipid regulators (bezafibrate, clofibric acid and metabolite), carbamazepine and trimethoprim are generally classified as harmful to aquatic organisms. Other antibiotics (ofloxacin, sulfamethoxazole, oxytetracycline, erythromycin) are mostly in the toxic range. However, there is also a lack of information regarding the synergistic impact of these chemicals, particularly at low concentrations over longer exposure periods.

EC pollution in the environment can be mitigated by processes such as ozonation, electrochemical oxidation, hydrogen peroxide/UV, Fenton degradation, and adsorption [28].

II.3. Advanced oxidation technologies used to remove emerging contaminants

Primary wastewater treatment is primarily aimed at removing suspended solids entering treatment plants and is generally ineffective in removing potentially harmful micropollutants. Micropollutants such as organic chemicals and pharmaceutical compounds are often too small or too dissolved in water to be effectively removed by primary treatment processes. In secondary treatment, a variety of processes are used, including dispersion, dilution, partitioning, biodegradation, and abiotic transformation. In general, during secondary treatment, micropollutants are not completely decomposed, which can lead to incomplete mineralization or the formation of by-products. However, several studies have shown that some of these molecules are not readily biodegradable, which may pose a problem in their effective treatment in wastewater treatment systems. Therefore, secondary and advanced treatment methods, such as adsorption, ozonation, photocatalysis, and others, are used to address these issues and reduce the presence of micropollutants in treated wastewater [2828. The elimination of micropollutants generally depends on the physico-chemical properties of the respective micropollutant and the treatment conditions applied in water treatment processes.

Advanced oxidation technologies (AOPs) are a set of well-established treatment methods that rely on the photocatalytic generation of strongly oxidizing radical species to degrade and destroy persistent pollutants. For more than two decades, heterogeneous photocatalytic AOP has been the focus of sustained research activity due to its efficiency in the complete destruction of pollutants, its nonselectivity, and the formation of nonhazardous products. Depending on their photochemical or non-photochemical characteristics, advanced oxidation processes can be classified as follows:

Table 2. 1 The most widely used advanced oxidation processes for the removal of organic pollutants.

No. crt.	Non-photochemical processes	Photochemical processes
1	Ozonation in alkaline medium	Ultraviolet (UVV) vacuum photolysis of water
2	Ozonation (O_3/H_2O_2)	UV/H_2O_2
3	The classic Fenton Fe^{2+}/H_2O_2	UV/O_3
4	Electro Fenton process	Photo-Fenton
5	Ultrasonic screen	Heterogeneous photocatalysis

II.4. The degradation mechanism of clofibric acid

The degradation mechanism of clofibric acid (CLF) is presented in figure 2.1 based on the proposed molecular structures of the secondary products.

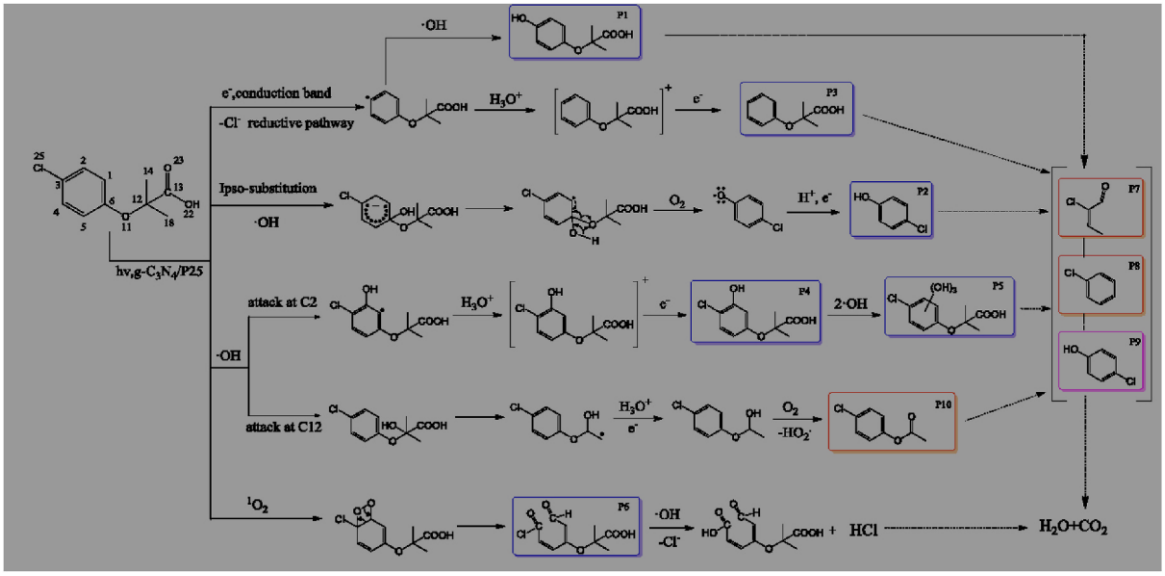

Figure 2. 1 The path of degradation of clofibric acid by photocatalysis [30].

II. 5. Partial conclusions

Environmental degradation is one of the most significant threats facing human communities today, and the findings suggest that one possible solution is to strengthen investment in promising technologies with high potential to remove emerging pollutants and contaminants. However, the results also highlighted that further research activities are mandatory to support the development of effective and cost-effective treatment technologies to reduce increasing environmental pollution and adverse human health effects, supporting a

coherent sustainability perspective aimed at towards improving the well-being of future generations and preserving the planet's life support systems.

CHAPTER III. RESEARCH OBJECTIVES AND METHODOLOGY

III.1. The objectives of the doctoral thesis

The main objective of the thesis is the green synthesis of some ZnO nanostructures in order to be used as a photocatalyst for the degradation of some emerging pollutants in water. ZnO nanostructures were obtained and tested in powder form, but also embedded in alginate matrices in order to identify sustainable solutions applied to water decontamination. It was opted for immobilization on a biopolymeric support, such as alginate, which is environmentally friendly and effective in water pollution reduction processes. This choice was driven by the nanometric dimensions of ZnO, which may pose a potential risk of uncontrolled release into the environment. The subject addressed is part of the principles of environmental protection and sustainability and the circular economy, by using a green method of synthesis, in which extracts from fruit waste are used. Also, the integration of ZnO nanostructures was carried out in biopolymer matrices, compatible with the environment, which have as the initial source of obtaining algae. The eco-materials thus obtained have been tested as photocatalysts for the decontamination of aqueous environments from emergent pollutants.

The chosen topic contributes directly to the development of the field of environmental engineering by: (i) *reducing the amount of waste from fruits* by valorizing them in green synthesis stages in order to obtain nanostructured eco-materials with photocatalytic properties; (ii) *decontamination of waters polluted with emergent contaminants* by photodegradation using environmentally friendly catalysts; (iii) *demonstrating and establishing the mechanisms underlying the physico-chemical processes* favoring the removal of emergent pollutants from water; (iv) *creation and development of a complex program* for the synthesis, characterization and testing of eco-materials with photocatalytic properties.

The research carried out during the doctoral internship led to the achievement of multidisciplinary results, involving knowledge from fields such as environmental protection and engineering, as well as materials science.

In order to achieve the main objective of the doctoral thesis, several scientific and technical objectives were taken into account: (i) the design and development of 3 types of ecological materials based on ZnO with a photocatalytic role synthesized by green methods, using as raw material extracts from grapefruit, pomelo and grape skins; (ii) presentation of

the concept of obtaining the 3 types of eco-materials with a photocatalytic role synthesized by encapsulating in a biopolymeric matrix, such as alginate, the 3 eco-materials mentioned above, thus reducing the risk of uncontrolled discharge into medium, using sodium alginate as raw material; (iii) defining and qualitatively and quantitatively evaluating the performances of the 6 ecological materials, by analyzing their structural, surface and chemical characteristics, regarding the ability to capture emerging pollutants from synthetic aqueous solutions; (iv) validation of the proposed concept by developing a comprehensive program of morphological, structural and surface properties characterization, with the aim of correlating this information with the assessment of the capture capacity of emergent pollutants from synthetic aqueous solutions; (v) confirming and validating the effectiveness of the materials in retaining emerging pollutants by applying specific kinetic and isotherm adsorption mechanisms, including investigations on the regeneration process.

Considering the bibliographic analysis, the research directions will focus on studying an optimal method of synthesis of these eco-materials with photocatalytic properties in order to degrade emerging contaminants from water.

III.2. Plan of experimental investigations

The experimental research was carried out in the research laboratories of the two universities as follows:

- The obtaining of eco-materials based on ZnO and those embedded in alginate matrices, with photocatalytic properties, but also the research on morphological and structural characterization was carried out within the Environmental Protection laboratories at the ECOMET Research and Expertise Center of the National University of Science and Technology POLYTECHNIC BUCHAREST.
- Testing the efficiency of ecological materials in photocatalytic processes, both under ultraviolet and visible light illumination conditions, using advanced oxidation methods was carried out in the chemistry laboratories of the École Nationale Supérieure de Chimie de Rennes (ENSCR) , Université de Rennes 1, France, Department of Chemistry and Process Engineering. The financing of the 3-month doctoral mobility (February-April 2022), carried out in France, was provided through the ERASMUS+ Program offered by the National University of Science and Technology POLITEHNICA BUCHAREST.

III.3. Research methodology

The research methodology was developed to synthesize three types of eco-friendly materials based on ZnO, using plant extracts and biopolymeric solid supports, which

subsequently integrate the three eco-friendly materials. These eco-materials have been developed with the aim of minimizing the risk of uncontrolled release into the environment due to their small size. The process of design, characterization and testing of ecological materials was oriented on the basis of existing knowledge in the specialized literature, regarding the current stage of development in this field. Different synthesis methods were investigated and the performances of the ecological materials were evaluated. The research methodology, planning and conduct of the experiments were developed and implemented within the Environmental Protection Laboratory of the ECOMET Center at UNSTPB. The doctoral research was structured according to Figure 3.1.

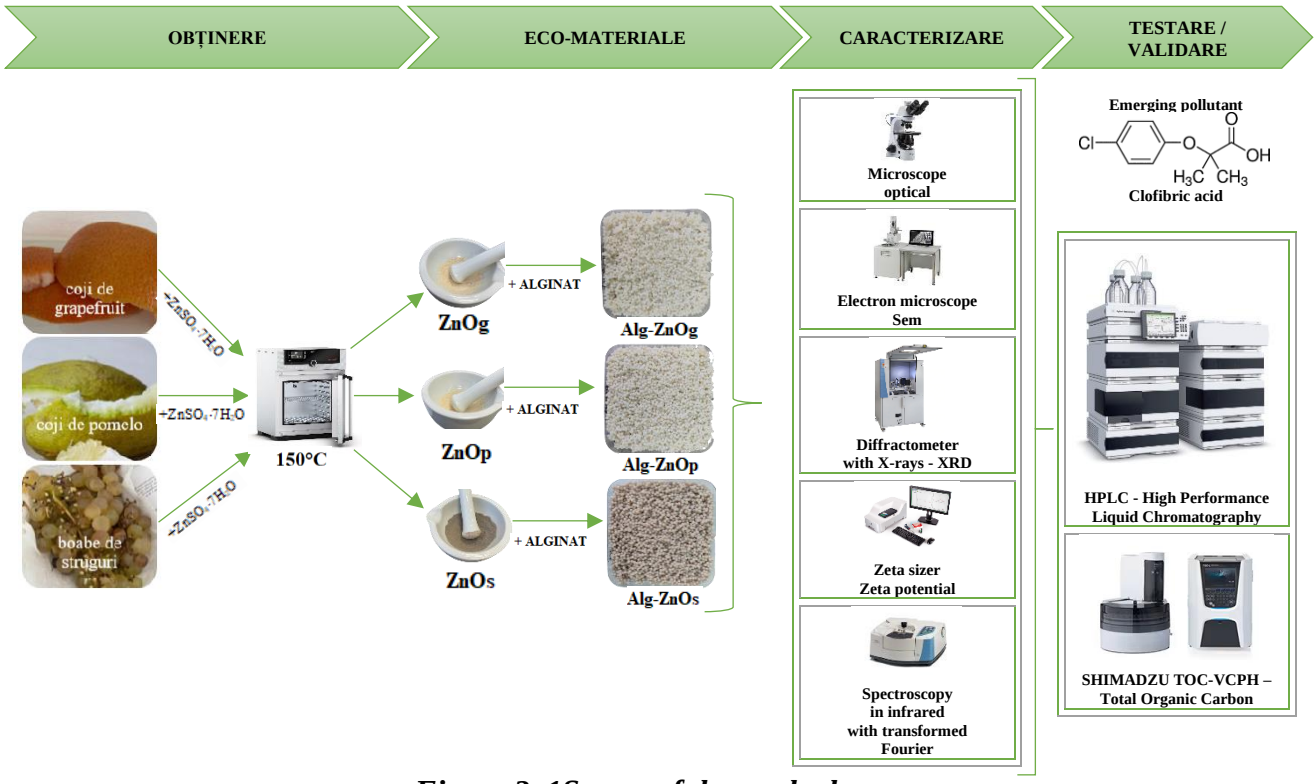

Figure 3. 1Stages of the work plan.

I II.4. Work methods and equipment used

The design of experiments in the thesis was designed and implemented using the equipment and methods detailed in Table 3.1.

Table 3. 1 Work methods and equipment used.

No. crt.	Work stages	Equipment / Laboratory instruments used
1.	**Obstruction and characterization of ZnO with grapefuit / pomelo peel extract (ZnOg / ZnOp)**	
1.	Weighing waste from grapefruit peels / pomelo peels	Laboratory glassware (watch glass) Analytical balance (Ohaus Explorer)
2.	Wash with distilled water	Laboratory glassware (Berzelius glass)
3.	Boil at 80 °C + magnetic stirring; 30 minutes	Magnetic stirrer with hot plate Laboratory glassware (Berzelius glass)
4.	Filtration	Whatman No. 1 filter paper

5.	Synthesis of ZnO with $ZnSO_4 \cdot 7H_2O$ and peel extract at 65 °C + magnetic stirring at 300 rpm, 3h	Magnetic stirrer with hot plate Laboratory glassware (Berzelius glass)
6.	Wash 7 times with distilled water	Laboratory glassware (Berzelius glass)
7.	Drying at 150°C	Laboratory oven (Memmert)
8.	Shredding + weighing	Laboratory glassware (pestle mortar) Analytical balance (Ohaus Explorer)
9.	Morphological, structural, surface and stability characterization	Olympus optical microscope (BX 51 M) Scanning electron microscope SEM (FEI, QUANTA 450 FEG) equipped with energy dispersive spectrometer (EDS) X-ray diffractometer (PANalytical, Model: X'Pert PRO MPD X) ZetaNanosizer (Malvern, Model: Zetasizer Nano ZSP) FTIR spectrometer (INTERSPECTRUM Estonia, Model: Interspec 200-X)
2.	**Preparation and Characterization of ZnO with Grape Seed Extract (ZnOs)**	
10.	Weighing waste grape berries	Laboratory glassware (watch glass) Analytical balance (Ohaus Explorer)
11.	Wash with distilled water	Laboratory glassware (Berzelius glass)
12.	MIXING	Laboratory glassware (Berzelius glass) Tefal blender
13.	Filtration	Laboratory glassware (Berzelius glass, filter funnels) Whatman No. 1 filter paper Buchner vacuum filtration system
14.	Synthesis of ZnO with $ZnSO_4 \cdot 7H_2O$ and grain extract at 60 °C + magnetic stirring at 300 rpm, 2h	Magnetic stirrer with hot plate Laboratory glassware (Berzelius glass)
15.	Wash 7 times with distilled water	Laboratory glassware (Berzelius glass)
16.	Drying at 150°C	Laboratory oven (Memmert)
17.	Shredding + weighing	Laboratory glassware (pestle mortar) Analytical balance (Ohaus Explorer)
18.	Morphological, structural, surface and stability characterization	Olympus optical microscope (BX 51 M) Scanning electron microscope SEM (FEI, QUANTA 450 FEG) equipped with energy dispersive spectrometer (EDS) X-ray diffractometer (PANalytical, Model: X'Pert PRO MPD X) ZetaNanosizer (Malvern, Model: Zetasizer Nano ZSP) FTIR spectrometer (INTERSPECTRUM Estonia, Model: Interspec 200-X)
3.	**Obtaining and Characterizing Classical ZnO (ZnO)**	
19.	Synthesis of ZnO with $ZnSO_4 \cdot 7H_2O$ + magnetic stirring at 300rpm, 2h	Magnetic stirrer with hot plate Laboratory glassware (Berzelius glass)
20.	Wash 7 times with distilled water	Laboratory glassware (Berzelius glass)
21.	Drying at 150°C	Laboratory oven (Memmert)
22.	Shredding + weighing	Laboratory glassware (pestle mortar) Analytical balance (Ohaus Explorer)
2. 3.	Morphological, structural, surface and stability characterization	Olympus optical microscope (BX 51 M) Scanning electron microscope SEM (FEI, QUANTA 450 FEG) equipped with energy dispersive spectrometer (EDS) X-ray diffractometer (PANalytical, Model: X'Pert PRO MPD X) ZetaNanosizer (Malvern, Model: Zetasizer Nano ZSP) FTIR spectrometer (INTERSPECTRUM Estonia, Model: Interspec 200-X)
4.	**Obtaining and characterization of Alg, Alg-ZnOg, Alg-ZnOp and Alg-ZnOs, system characterization**	

24.	Obtaining Alg: dissolving Na Alginate (1%) in hot distilled water, stirring, 90°C, 4 h, 200 rpm. Obtain Alg-ZnOg 1:1, Alg- ZnOp 1:1, ZnOs 1:1: ZnOg / ZnOp / ZnOs powder dispersion in AlgNa, dripping into a 2% $CaCl_2$ bath.	Reagents: Sodium alginate, BioChemica, $CaCl_2$ 2% Laboratory glassware Analytical balance (Ohaus Explorer) Magnetic stirrer with hot plate Ultrasonic device Laboratory oven (Memmert) Pumping system TL-BM-300
25.	Morphological, structural, surface and stability characterization	Olympus optical microscope (BX 51 M) Scanning electron microscope SEM (FEI, QUANTA 450 FEG) equipped with energy dispersive spectrometer (EDS) FTIR spectrometer (INTERSPECTRUM Estonia, Model: Interspec 200-X)
5.	**Testing the photocatalytic degradation capacities of the synthesized materials**	
26.	The photocatalysis process	Experimental set consisting of: - Berzelius glass of 600 ml; - 200 ml of CLF solution previously prepared in a 1L volumetric flask by diluting a known amount of pollutant in ultrapure water; - Tube with compressed air to keep the solution homogeneous throughout the degradation; - Plastic tube for sampling; - Magnetic stirrer for mixing the solution throughout the degradation; - Eco-material with photocatalytic role; - Glass tube – support for the UV lamp, which is placed inside the solution; - UV lamp Philips PL-L 24W/10/4P, with a maximum emission at 227 nm (turns on for one hour before handling) and is placed in the glass tube after one hour; - Aluminum foil; - Timer.
27.	Efficiency of photocatalysis	High Performance Liquid Chromatography (HPLC); pH meter Hanna HI 19812-5 pH/C/EC/TDS; SHIMADZU TOC-VCPH.

III.5. Materials

The photocatalysts used in the experimental system are synthesized by green methods and the obtaining process is described in detail in Chapter IV. OBTAINING PHOTOCATALYTIC MATERIALS.

Zinc sulfate heptahydrate (CAS 7446-20-0) with the molecular formula $ZnSO_4 \cdot 7H_2O$ and sodium hydroxide (CAS 1310-73-2) with the molecular formula NaOH are the reagents used for the synthesis of zinc oxide and were purchased from CHIMOPAR TRADING Romania.

The fruits and peels used for the preparation of the extracts are purchased commercially in Romania.

Sodium alginate salt having the molecular formula $C_6H_7O_6Na$ was purchased from PanReac AppliChem.

Anhydrous calcium chloride with the molecular formula $CaCl_2$ was purchased from CHIMREACTIV SRL Romania.

Clofibric acid (CLF) is a herbicide and is also a pharmaceutical compound. CLF has the chemical structure shown in figure 3.2 and is one of the recalcitrant pharmaceutical compounds observed as an environmental pollutant in recent times.

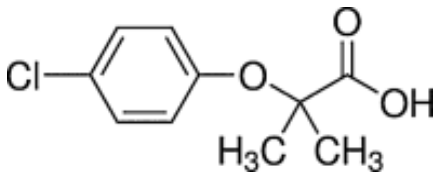

Figure 3. 2Chemical structure of clofibric acid [31].

CLF is a metabolite of clofibrate and serves as a lipid regulator [32]. As a medicine, it serves as an anti-cholesteremic, anti-lipemic and antineoplastic agent. Due to its structural complexity and the intermediates involved, biological decomposition is ineffective in removing this chemical compound. Therefore, this drug has a significant lifetime in the environment. To date, various techniques have been investigated to extract this molecule from wastewater, including biodegradation, photodegradation, and advanced oxidation processes. In response to this problem, advanced oxidation methods (AOPs) have emerged as a potentially powerful approach to transform pollutants into harmless substances.

Clofibric acid (CLF) is a white solid and was purchased from Sigma-Aldrich France. The basic properties of CLF are summarized in Table 3.2:

Table 3. 2Basic properties of clofibric acid.

property	**stock**
CAS number	882-09-7
IUPAC number	2-(4-Chlorophenoxy)-2-methylpropanoic acid
Chemical formula	$C_{10}H_{11}ClO_3$
Molar mass	214.64 g/mol
Specific gravity (at 20°C)	1.3
Solubility in water (at 20°C)	583 mg/l
pk	3.18
LogKow _	2.6
Melting point	118.5°C
Boiling point	324.1°C

Pentoxifylline (PTX) (CAS 6493-05-6) is a drug used to treat muscle pain, it has the chemical formula $C_{13}H_{18}N_4O_3$ and the IUPAC number 3,7-dimethyl-1-(5-oxohexyl)-3,7-dihydro-1H-purine-2,6-dione and was purchased from Sigma-Aldrich France.

Chloroxylenol (PCMX) (CAS 88-04-0) is an organic antiseptic compound and a disinfectant used to disinfect skin and surgical instruments, it has the chemical formula C_8H_9ClO and the IUPAC number 4-Chloro-3,5-dimethylphenol and a was purchased from Sigma-Aldrich France.

Acetonitrile (CAS 75-05-8, HPLC Gradient Grade, Purity 99.99%), Formic Acid (CAS 64-18-6, Purity > 99.5%, Optima LC/MS Grade) and Potassium Hydrogen Phthalate

used as standard in TOC quantification (CAS 877-24-7, purity ≥ 99.95%, BioXtra) were purchased from Fisher Chemical and Sigma-Aldrich.

For all experiments, solutions were prepared using ultrapure water with a resistivity of 18.2 MΩ·cm at 298 K, which was produced by an ELGA Option-Q DV 25 water purification system.

III.6. Morphological, structural and surface characterizations

A thorough analysis of the morpho-structural characteristics of eco-materials obtained from waste, as well as of those integrated in biopolymer matrices, was carried out. This analysis was carried out through an exhaustive research program that highlighted the parameters with impact on the retention processes of emergent compounds from aqueous solutions, using the developed eco-materials. The characterization techniques used included optical microscopy (OM) and scanning electron microscopy (SEM) in combination with energy dispersive spectroscopy (EDS), X-ray diffraction (XRD), zeta potential and pHpzc analysis, as well as infrared spectroscopy with Fourier transform (FTIR) with attenuated total reflection (ATR) technique.

Further, following the detailed characterization of these eco-materials, either in plain form or integrated into polymer matrices, they were tested using synthetic aqueous solutions containing emergent contaminants. In these tests, the optimal contact times for various amounts of material were evaluated. The values recorded before and after the interaction with these materials were analyzed, thus highlighting their ability to degrade certain types of pollutants. High Performance Liquid Chromatography (HPLC) and TOC analysis were used to analyze the results.

By analyzing the investigated parameters, data sets were generated that facilitated the selection of the most efficient eco-material, suitable for use in water purification systems, in the form of a filter material. The techniques used in this process are detailed below.

III.7. Methods of detection of analyzed pollutants

III.7.1. High Performance Liquid Chromatography (HPLC)

HPLC is essentially an improvement on the high-performance liquid chromatography technique. Instead of letting the solvent pass through the column under gravity, in HPLC, it is forced through a high pressure of up to 400 atmospheres, which speeds up the process considerably. All chromatographic methods, including HPLC, are based on the same fundamental principle: the separation of a sample into its individual components due to

differences in the relative affinity of the various molecules for the mobile phase and the stationary phase used in the separation process.

An HPLC system consisting of a WATERS 600 pump, a WATERS 717 autosampler and a WATERS PDA 996 detector was used to determine the concentration of pollutants. This system operates using the Empower software. The column used is a WATERS C18 Symmetry® with dimensions of 4.6 x 250 mm and silica particles of 5 μm, produced in Ireland.

III.7.2. Analysis of OCD

The determination of carbon concentration in the analyzed samples was carried out using the SHIMADZU TOC-VCPH system. The components of the analytical system include:

- Autosampler ASI-V SA for sample handling;
- VCPH TOC analyzer using catalytic oxidation to determine carbon content.

There are two main types of carbon in water: organic carbon and inorganic carbon. Organic carbon (TOC) is bonded to hydrogen or oxygen to form organic compounds. On the other hand, inorganic carbon (IC or TIC) represents the structural component of inorganic compounds, such as carbonates and carbonate ions. In total, the two forms of carbon are referred to as total carbon (TC), and the relationship between them is expressed by the formula TOC = TC - IC.

III.8. The working protocol applied for testing the photocatalytic performances of the synthesized eco-materials

For the evaluation of the obtained eco-materials, a laboratory facility developed and built within the doctoral program was used. The experimental setup is detailed in Table 3.1.

In all experiments performed, a measured amount of CLF is dissolved in a 1 liter volumetric flask under magnetic stirring for 15 hours using ultrapure water. To prevent degradation of the compound by exposure to light during the stirring process, the flask was covered with an aluminum foil.

The photocatalytic degradation of CLF was performed in a laboratory environment in a batch system at room temperature with an ultrapure water solution of set concentrations of CLF that was brought into contact with each synthesized catalytic eco-material selected for testing in a 600 ml glass reactor. Clofibric acid was weighed using a precision balance (with an accuracy of 10-2 g ± 0.005 g). The pH has not been adjusted. At room temperature, the solution has a temperature between 25 and 27°C. After dissolving the clofibric acid for 15 hours, an amount of 200 ml was transferred to the reactor. The solution was stirred with

the help of a magnet and air blown through the plastic tube for 1 h with ZnO added to allow complete adsorption of CLF on the ZnO surface. The adsorption process was monitored at regular time intervals and overnight with a stirring speed of 4000 rpm. The optimal adsorption time was determined to be approximately one hour. During this period, the UV lamp was activated at the maximum light level to reach the optimal temperature and light intensity. The value of the maximum luminous intensity was 5.56 mW/cm ^{2} and the wavelength of 227nm. Once the adsorption process was complete, the UV lamp was inserted into a glass tube in the center of the reactor. At the beginning of the adsorption process, an aeration tube and a magnetic bar were placed to ensure complete mixing of the CLF and to effectively depress the catalyst. Stirring and aeration were maintained throughout the reaction to maintain a homogeneous suspension. An aluminum foil was used to cover the walls of the reactor to minimize the influence of external radiation. Also, a plastic tube was placed in the reactor for easy sampling. Samples of 2 ml of the solution containing CLF were taken with a syringe through the plastic tube at certain time intervals. Subsequently, these samples were subjected to centrifugation to separate the catalyst particles. After the samples were centrifuged for 10 min at a speed of 4000 rpm using a Jouan C412 centrifuge, the suspensions were passed through the CROMAFIL Xtra H-PTEE filter with a porosity of 0.45 μm using a syringe. Subsequently, residual CLF concentrations were analyzed.

During each experiment, a total of 14 samplings were performed, including the first sampling at the beginning of the experiment, before turning on the UV lamp, then a sampling after one hour of equilibration, i.e. exactly at the moment of turning on the UV lamp, and subsequently at every 30 minutes for 6 hours.

To evaluate the effectiveness of the synthesized oxide eco-materials in the study of heterogeneous photocatalytic degradation kinetics, 12 parameters were monitored to track their impact , as follows :

• choosing the optimal catalyst for the effective degradation of CLF, testing first the 4 types of powdered ZnO (ZnOp, ZnOg, ZnOs and ZnOc), and then the 4 eco-materials based on alginate and ZnO (Alg-ZnOp, Alg- ZnOg, Alg-ZnOs, Alg);

• the comparative study of photolysis, photocatalysis and adsorption;

• degradation of different pharmaceutical pollutants (clofibric acid, pentoxifylline and chloroxylenol);

• variation of the initial concentration of CLF in the range: 5 mg/L, 10 mg/L, 30 mg/L, 60 mg/L and 100 mg/L;

• variation of the initial concentration of ZnO in the range: 20 mg/L, 50 mg/L, 100 mg/L, 250 mg/L, 500 mg/L, 1000 mg/L, 2000 mg/L;

• luminous flux intensity: minimum, average and maximum luminous flux;

• the effect of different water matrices (ultrapure water, bottled water, tap water, well water);

• the effect of the initial pH of the solution (natural pH = 5, adjusted pH = 4, 6, 8, 10);

• the effect of inorganic anions (HCO_3^-, SO_4^{2-}, Cl^-);

• the effect of inorganic cations (Na^+, Mg^{2+}, Ca^{2+});

• the effect of some inhibitors (isopropanol and tempol);

• recycling cycles of synthesized eco-materials;

To perform a comparison between the different studies, each parameter was varied individually at a given time. Subsequently, the percentage reduction in CLF concentration at six hours of irradiation was calculated to evaluate the efficiency according to each changed parameter. This is a useful way to determine the influence of each parameter on the photocatalytic degradation process of CLF.

III.9. Photodegradation and kinetics tests

The yield can be calculated as follows:

$$\eta = \frac{m_i - m_f}{m_i} * 100 \quad (20)$$

To calculate the degradation percentage of the studied pollutant, the formula given by relation (21) was used:

$$(\%)eliminare = \frac{[CLF]_f - [\mathrm{CLF}]_{iUV}}{[CLF]_f} x100 \quad (21)$$

$[CLF]_{iUV}$ – represents the initial concentration of CLF from the moment the UV lamp is turned on, obtained using HPLC;

$[CLF]_f$ - represents the final concentration of CLF obtained by HPLC.

To calculate the adsorption capacity of ZnO, we used the following formula, given by relation (22):

$$\text{Capacitatea de adsorbție} = \frac{[CLF]_i - [CLF]_{iUV}}{\mathrm{m}} \quad (22)$$

$[CLF]_{iUV}$ – represents the initial concentration of CLF from the moment the UV lamp is turned on, obtained using HPLC;

$[CLF]_i$ – represents the initial concentration of CLF from the moment of starting the experiment obtained with the help of HPLC;

m – represents the mass of zinc oxide (in grams).

By watching how the concentration of the pollutant changes over time, we can calculate its initial rate of degradation. This allows us to observe a direct correlation between the inverse of the initial concentration of the pollutant and the inverse of the degradation rate.

Understanding the mechanism of pollutant degradation can be facilitated by kinetic studies. Essentially, the Langmuir–Hinshelwood (LH) reaction is surface dependent and is expected to have an increased reaction rate as the irradiation period is increased. This is because as the irradiation time increases, the amount of remaining organic substrate decreases, leading to a greater availability of the catalyst surface for the reaction. The entire decomposition achieved is coupled with a zero decay rate.

In a photocatalytic process, the degradation rate is generally described by the Langmuir-Hinshelwood (LH) equation [33]:

$$-r = \frac{dC}{dt} = K_{app} * C = -\frac{k_r KC}{1+KC} \quad (23)$$

where $-r$ - represents the speed of the photocatalytic reaction, C - represents the concentration of the pollutant at time t, K_{app} - the rate constant for pseudo-reaction of the first order (min^{-1}), k_r - the specific rate constant for pollutant oxidation (mg /L/min), K - adsorption equilibrium constant (L/mg). Integrating equation (23) yields:

$$\ln\left(\frac{C_0}{C}\right) = K_{app} * t \quad (24)$$

where C_0 - represents the initial concentration of the pollutant and t - reaction time (min).

The kinetics is an obvious first-order reaction for low-concentration solutions:

$$r = -\frac{dC}{dt} = k_r KC = k_{app} C \quad (25)$$

The linearization of equation (25) represents the first-order kinetics:

$$-\ln\frac{C}{C_0} = k_{app} t \quad (26)$$

The following equation can be used to calculate the initial velocity r_0:

$$r_0 = k_{app} C_0 \quad (27)$$

The LH model rate constants (kr) and adsorption (K) were determined using the initial concentrations:

$$r_0 = k_r \frac{KC_0}{1 + KC_0} \quad (28)$$

The K value can be calculated from the linearization of Equation (23) and the graphical representation of 1/r vs. $1/C_0$:

$$\frac{1}{r_0} = \frac{1}{k_r} + \frac{1}{k_r KC_0} \quad (29)$$

CHAPTER IV. OBTAINING ECO-MATERIALS WITH PHOTOCATALYTIC ROLE

Based on the information from the first part of this study, which presents a literature review, experiments were carried out to find solutions for the recovery of vegetable waste, such as grapefruit peels, pomelo peels and grape seeds. These wastes were obtained from the consumption of these fruits and were chosen because of their high flavonoid content and their potential to be transformed into eco-materials with photocatalytic properties for the removal of pollutants from water. Experiments included characterizing these wastes and testing them to identify effective ways of recovery.

In line with the idea of the circular economy, which is committed to minimizing the generation of waste, the process of transforming a waste into a value-added product has a positive impact on the environment. This translates into reducing the need for raw materials, decreasing carbon emissions produced from plant sources, avoiding landfilling, and ultimately conserving natural resources.

IV.1. Synthesis of ZnO nanoparticles using plant extract

The obtaining methods described below are applied in the Ecology Laboratory within the Eco-Metallurgical Research and Expertise Center of the Faculty of Materials Science and Engineering, National University of Science and Technology POLITEHNICA BUCHAREST.

The plant extracts used were of three types, two of which were from citrus peel waste and one from grape fruit waste. The obtained extracts were used for the green synthesis of ZnO nanoparticles, adopting a simple technique.

The principle of obtaining zinc oxide is based on a precipitation reaction of heptahydrated zinc sulfate precursors in an alkaline environment using the extract from peels or fruits as a reducing medium. The method is known in the literature as the bioreduction method .

IV.1.1. Synthesis of ZnO nanoparticles using grapefruit extract

The synthesis and stabilization of ZnO nanoparticles using the outer peel extract of Citrus Paradisi (grapefruit) by the bioreduction method was studied in detail; these nanoparticles were further investigated as catalysts for the degradation of persistent organic pollutants. These citrus fruits, namely grapefruit (C. paradisi) and pomelo (C. maxima) contain relatively high levels of bioactive compounds of interest, are unique in their sensory quality of sweet and sour taste, with red or yellow pigment in the juice vesicles. Flavonoids, limonoids, carotenoids, furocoumarins and organic acids are the most important bioactive

components found in grapefruit and pomelo [34]. The efficiency of obtaining grapefruit extract was 84% applying equation (20) from subchapter III.9.

ZnOg (ZnO-grapefruit) nanoparticles were prepared using a 3 mM $ZnSO_4 \cdot 7H_2O$ (aq) solution. In a typical preparation, 30 mL of aqueous Citrus paradisi peel extract was added to 30 mL of 3 mM $ZnSO_4 \cdot 7H_2O$, and the pH was adjusted to 11 using 3 mM NaOH. The mixture was stirred at 300 rpm for 3 hours at 75°C and kept for observation until the color changed. The formation of ZnO nanoparticles is evidenced by the color change from bright orange to milky orange.

The resulting ZnO nanoparticles were separated by settling overnight, and the next day they were washed five times with distilled water, subsequently dried in a hot air oven at 100°C and then calcined at 150°C for 1 hour. After calcination, the resulting nanoparticles were mortared in a pestle mortar. The efficiency of obtaining zinc oxide using grapefruit extract was 68%, applying equation (20) from subchapter III.9.

IV.1.2. Synthesis of ZnO nanoparticles using pomelo extract

The same process was used to prepare ZnOp nanoparticles (ZnO-pomelo), using Citrus maxima extract.

The efficiency of obtaining zinc oxide using pomelo extract was 72% applying equation (20) from subchapter III.9.

IV.1.3. Synthesis of ZnO nanoparticles using grape extract

Zinc oxide nanoparticles were also synthesized using a reducing and stabilizing agent from grape (Vitis vinifera) aqueous extract without any poisonous or unsafe chemicals, additives or promoters, and without any soluble or harmful organic agent.

Grape (Vitis vinifera) extract is rich in phytochemicals such as polyphenols, flavonoids and catechins, all of which can help reduce the metallic form of gold and silver salts. Grape extract has demonstrated remarkable efficacy as a reducing agent for the selective reduction of ketone and nitro compounds in addition to the creation of metal nanoparticles [35]. Several studies show that grape extract has great potential as a reducing agent. Phytochemicals in grape extract have significant therapeutic value while also being environmentally friendly, making them an attractive alternative to standard harmful abatement agents.

To prepare the aqueous extract of grapes, 400 grams of grapes were separated from the twigs and then washed with deionized water numerous times to remove dust, then crushed using a mixer in 400 mL of distilled water until the mixture was homogeneous. A brick orange colored solution was obtained after filtering the extract using Whatman No. 1 paper .

By mixing 400 g of grape seeds and 400 mL of water, a quantity of 680 mL of extract and 120 g of waste was obtained. The efficiency of obtaining the grape extract was 85% applying equation (20) from subchapter III.9.

ZnOs nanoparticles (ZnO-grapes) were synthesized using different mass ratios of plant extract and zinc sulfate to determine the optimal ratio. So, for the first synthesized eco-material (ZnOs 1:2) 20 ml of 1 mM $ZnSO_4 \cdot 7H_2O$ (water) solution and 40 ml of grape extract were used , and to reach pH 11 , 1 mM NaOH was added during mixing. For the second eco-material synthesized (ZnOs 1:1) 20 ml of 1 mM $ZnSO_4 \cdot 7H_2O$ solution and 20 ml of grape extract and 1 mM NaOH for pH 11 were used. The third eco -material (ZnOs 2:1) was synthesized with 40 mL of 1 mM $ZnSO_4 \cdot 7H_2O$ solution (aqueous) and 20 mL of grape extract, and also 1 mM NaOH was added for pH 11. The mixture was stirred at 300 rpm for 2 hours and continuously maintained at 60°C. The color changed from brick orange to milky cream and thus the formation of ZnO-NPs was proved. The resulting ZnO nanoparticles were separated by settling overnight, and the next day they were washed five times with distilled water and dried in a hot air oven at 100°C, then calcined at 150°C for 1 hour . After calcination, the resulting nanoparticles were mortared in a pestle mortar. The efficiency of obtaining zinc oxide using grape extract was 68%, applying equation (20) from subchapter III.9.

IV.1.4. Synthesis of classical ZnO nanoparticles

Zinc oxide nanoparticles without extract were also synthesized for comparison. The same preparation method was used for their synthesis.

IV.2. Synthesis of eco-materials with photocatalytic properties based on Alginate and ZnO

Equivalent amounts of zinc oxide powder (ZnO) and sodium alginate salt powder (Alg) were mixed to prepare sodium alginate zinc oxide (Alg-ZnO) spheres. The resulting mixture was sonicated for 30 minutes to obtain a homogeneous 1% aqueous solution.

Alg spheres with ZnO were obtained by dropping the resulting suspension into a 2% calcium chloride solution. The exposure time in the $CaCl_2$ crosslinking solution was 24 hours. The obtained eco-materials were subjected to additional operations, which include filtering, washing with distilled water and drying at room temperature.

Three types of eco-materials based on sodium alginate and zinc oxide (Alg-ZnO) were synthesized using three different types of ZnO with plant extracts, namely: Alg-ZnO-grapefruit (Alg-ZnOg), Alg -ZnO-pomelo (Alg-ZnOp) and Alg-ZnO-grape (Alg-ZnOs).

For comparison, sodium alginate spheres without zinc oxide were also synthesized. The same method described above was used for the preparation of alginate spheres.

IV.3. Partial conclusions

In the green synthesis, parameters such as the concentrations of the plant extract as well as the zinc source, as well as the pH of the solution play a major role on the final properties and characteristics of the NP-ZnO obtained by this method. Although ZnO-type materials, obtained by ecological methods, show promising results, the small size of the particles determined the research of their behavior when integrated in alginate-type polymer matrices. By using alginate as the embedding material, greater stability of the ZnO material can be achieved.

While alginate-based composites typically exhibit improved physical/mechanical properties over pure alginate spheres, the biocompatibility of alginate coupled with novel properties of encapsulated materials often provide synergistic functionalities of new derivatives. Among these are the ease of separation and the reduced risk of the encapsulated materials being lost to the environment. Thus, the incorporation of ZnO NPs as a photocatalyst in an alginate polymer matrix is a new approach in the green synthesis of photocatalysts, offering improved properties.

CHAPTER V. CHARACTERIZATION OF PHOTOCATALYTIC ECO-MATERIALS

V.1. Morphological, structural and surface characterizations of ZnO samples synthesized with plant extract

V.1.1. Optical microscopy

The nanoparticles obtained by the green method were characterized using the optical microscope at 50x magnification, as shown in Figure 5.1.

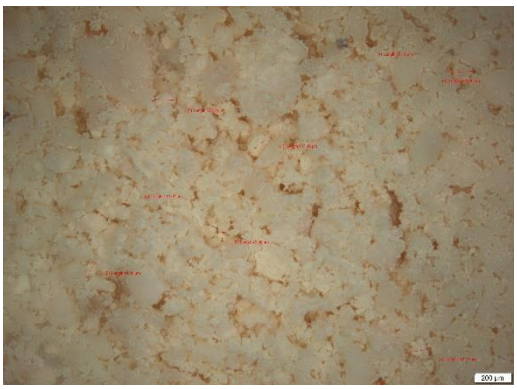

(a)

(b)

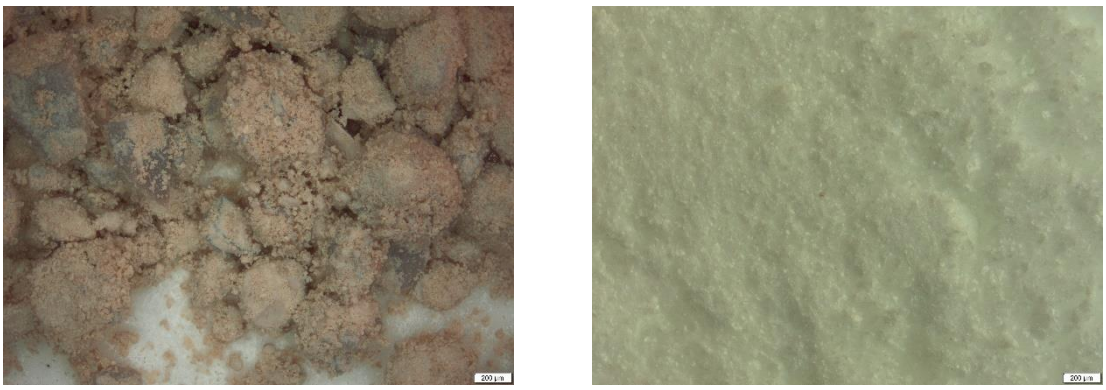

(b) ***(d)***

Figure 5. 1Images obtained by optical microscopy of ZnO samples at 50x magnification; (a) ZnOg; (b) ZnOp; (c) ZnOs; (d) ZnOc.

It can be observed that the sizes of ZnOc and ZnOg are located in the range of 50 – 150 nm, which are characteristic of nanoparticles. In contrast, the sizes of ZnO-pomelo and ZnO-grape are in the range of 100–500 nm, which means that the synthesis method should be improved. However, the nanoparticles retain their spherical configuration, which is a common feature of nanoscale ZnO particles.

V.1.2. SEM microscopy

The eco-materials based on ZnO obtained by green synthesis were characterized and investigated from the point of view of morpho-structural aspects, the structure, purity and dimensions obtained were analyzed in order to validate the experimental results regarding their use as photocatalysts. Thus, with the help of the scanning electron microscopy (SEM) technique, coupled with energy dispersive spectrometry (EDS) , the main aspects of the surface of the eco-materials as well as the type and distribution of the elements in the analyzed samples were identified. Initially, the 3 samples of ZnO obtained from fruit waste (ZnOg, ZnOp, ZnOs) and 1 sample of simple alginate were analyzed in order to compare with the samples containing ZnO incorporated in biopolymer matrix of Alg. Based on the results obtained, it was found that the sample obtained from grapefruit extract is the most effective in photocatalytic degradation, so figure 5.2 shows the morphology of the ZnOg sample, at magnifications of 100000x, where well-defined aspects of the ZnO nanoparticles, with sizes which varies in the range of 20 – 78 nm, the average size of the particles being about 57 nm. The EDS spectrum indicates the presence of Zn and O as main elements in the analyzed sample.

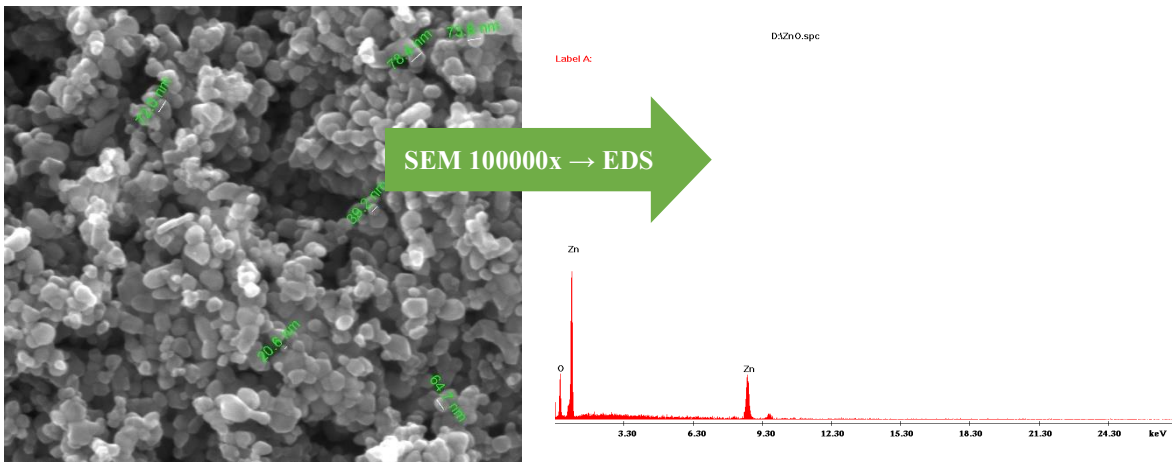

Figure 5. 2 Appearance of ZnOg sample at 100,000x and EDS elemental analysis.

V.1.3. XRD analysis

The presence of zinc oxide compounds in the analyzed samples (ZnOg) is confirmed by the diffractogram obtained (figure 5.3).

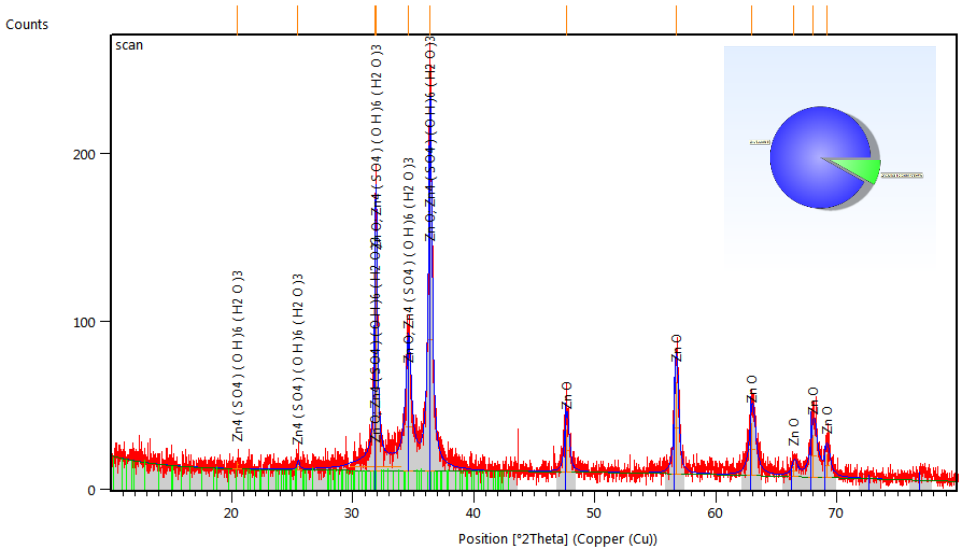

Figure 5. 3 Diffractogram and quantitative evaluation for ZnOg.

The presence of ZnO in majority proportion is quantitatively confirmed. We can observe a percentage of 92% zinc oxide and 8% sulfate of zinc heptahydrate totally unreacted by the bioreduction method.

Zinc oxide obtained from grapefruit extract is crystallized in the hexagonal system having the main maximum at 36,100 2Theta according to database reference 01-079-0208. The average crystallite size was determined using the Debye-Scherrer formula, its value being 22.60 nm.

Also, the presence of zinc oxide compounds in the ZnOp samples can be observed in the following diffractogram (figure 5.4):

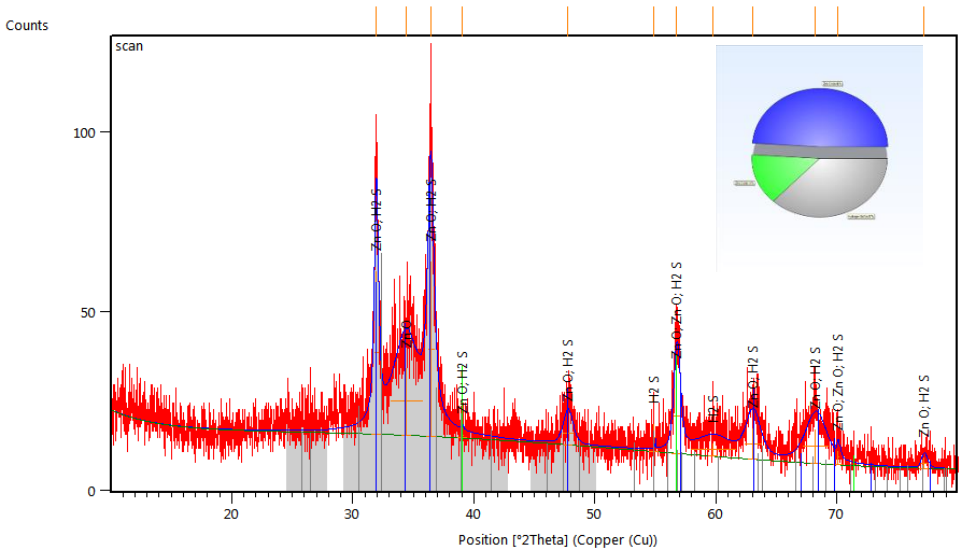

Figure 5. 4 Diffraction pattern and quantitative evaluation for ZnOp .

It also quantitatively confirms the presence of ZnO in the majority proportion. We can see a percentage of 63% zinc oxide and 37% unreacted hydrogen sulfate.

Zinc oxide obtained from pomelo extract is crystallized in 2 forms in the cubic system having the main maximum at 57,359 2Theta and in the hexagonal system having the main maximum at 36,672 2Theta according to the database with reference 01-080-4983, respectively 01-078-4604 . Using the Debye-Scherrer formula, the average size of the crystallites was calculated, the result being 8.29 nanometers.

Zinc oxide nanoparticles with grape extract (ZnOs) were also analyzed, and the presence of zinc oxide compounds can be seen in the following diffractogram (figure 5.5):

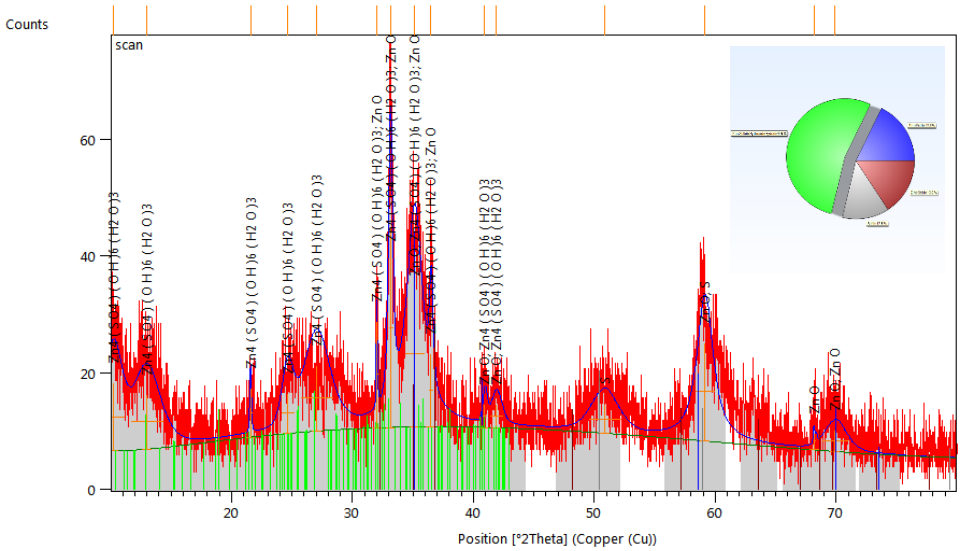

Figure 5. 5 Diffraction pattern and quantitative evaluation for ZnOs.

We can observe a percentage of 33.6% zinc oxide, 12.9% sulfur and 53.5% total unreacted zinc sulfate heptahydrate by the bioreduction method.

The zinc oxide obtained from the grape extract is crystallized in 2 forms in the cubic system having the main maximum at 34.581 2Theta and in the hexagonal system having the main maximum at 36.358 2Theta according to the database with reference 01-077-9355, respectively 01-079-0205 . Using the Debye-Scherrer equation, the average crystallite size was calculated, obtaining a value of 20.57 nm.

oxide nanoparticles without extract (ZnOc) were also analyzed, and the presence of zinc oxide compounds can be seen in the following diffractogram (figure 5.6):

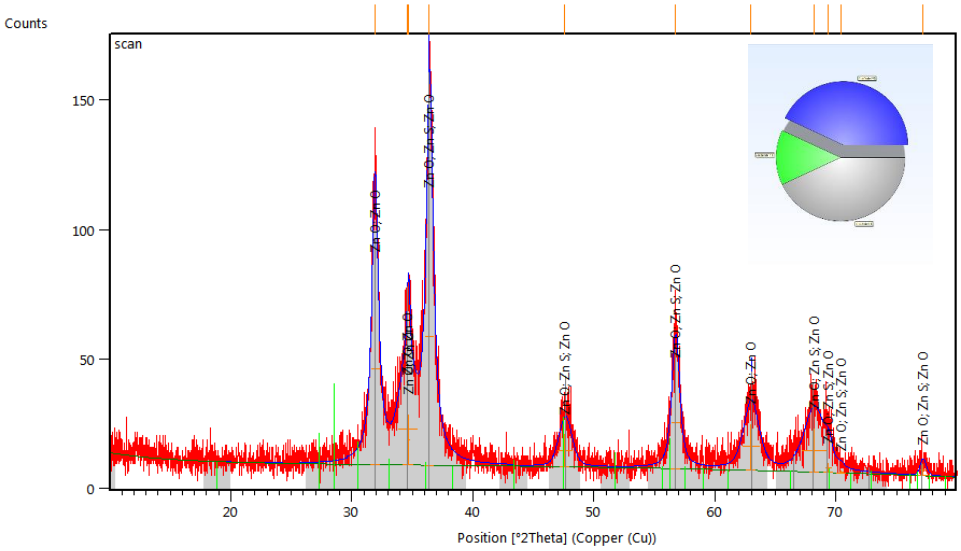

Figure 5. 6 Diffraction pattern and quantitative evaluation for ZnOc.

The presence of ZnO in majority proportion is also quantitatively confirmed . We can observe a percentage of 86% zinc oxide, 14% zinc sulfate totally unreacted by the bioreduction method.

The zinc oxide obtained by the classical method is crystallized in a hexagonal system having the main maximum at 36.247 2θ according to the database with reference 01-079-9878, respectively 01-078-4493. The average crystallite size was determined using the Debye-Scherrer formula, its value being 24.21 nm.

V.2. FTIR analysis for eco-materials synthesized with plant extract

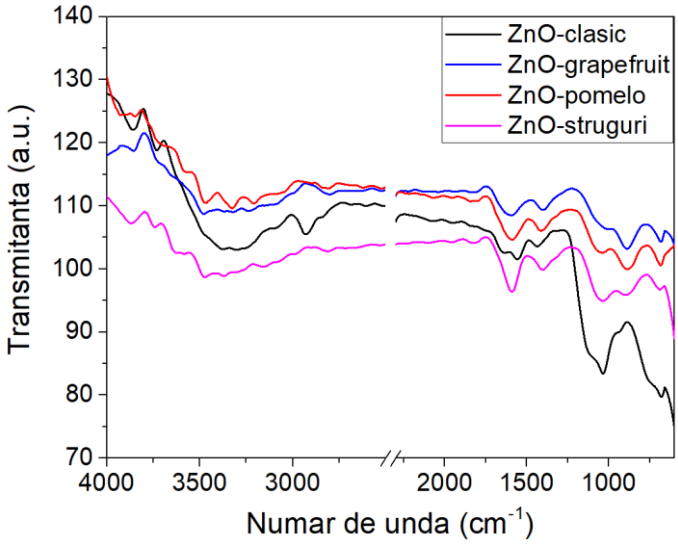

Figure 5. 7 Analysis of FTIR spectra for the 4 types of ZnO obtained by green synthesis.

The four materials prepared by classical synthesis and green synthesis with grapefruit, pomelo and grape extract were investigated from the structural point of view and the functional groups present with the help of ATR-FTIR analysis in the range 4000-600 cm^{-1}. The stretching vibrations of the -OH groups show an absorption maximum for all materials around 3300 cm^{-1}, the symmetric and asymmetric stretching vibrations specific to the -CH groups from the aliphatic groups are present at 2930 and 2838 cm^{-1} for classic ZnO, while for the materials prepared by green synthesis peaks are observed only at the wave number 2800 cm^{-1}. The absorption peaks at 1641, 1565 and 1440 cm^{-1} are attributed to the stretching vibrations of C=O, C=C and CC bonds respectively [36]. The stretching vibrations of the Zn-OH bonds are highlighted in the materials by the absorption peaks highlighted around 680 cm^{-1} .

V. 4. Morphological, structural and dimensional characterizations of Alg, Alg-ZnOg, Alg-ZnOp and Alg-ZnOs samples

V.4.1. Optical microscopy

The samples of simple alginate without zinc oxide but also the samples of ZnO incorporated in alginate matrix were analyzed microscopically, at 50x magnification, as shown in figure 5.8.

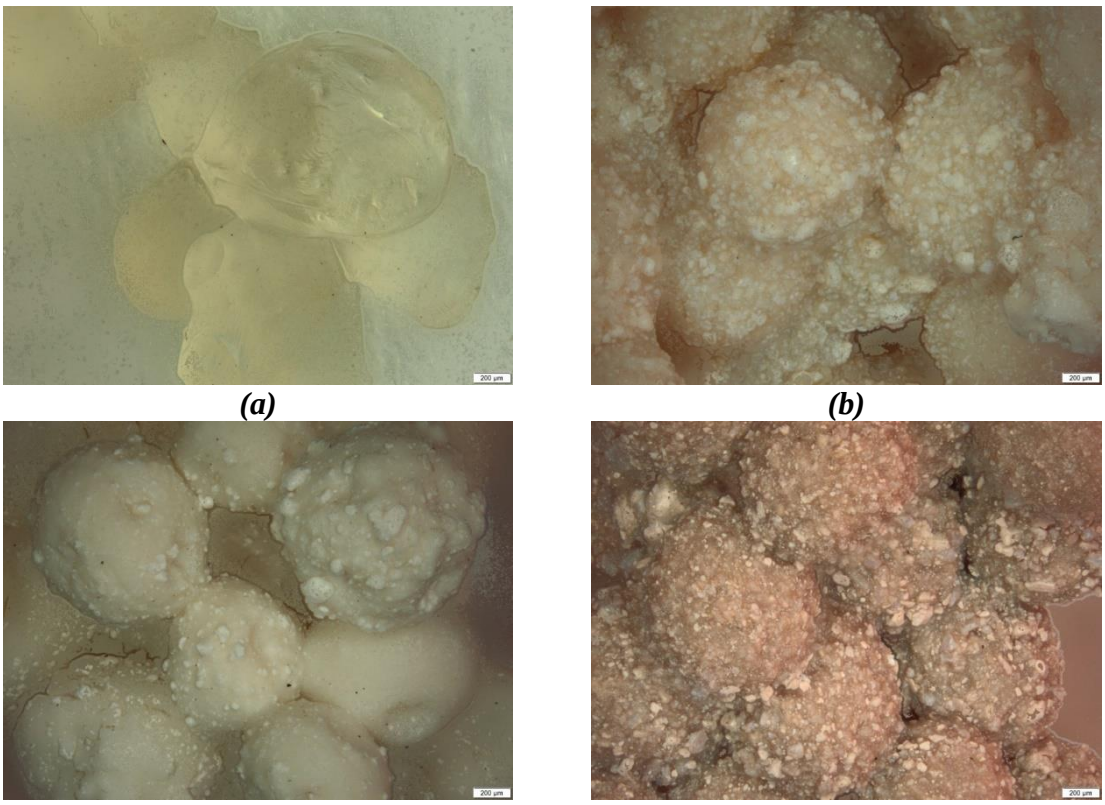

(a) ***(b)***

(b) ***(d)***

Figure 5. 8 Optical microscopy images of (a) Alg 1%, (b) Alg-ZnOg, (c) Alg-ZnOp and (d) Alg-ZnOs samples at 50x magnification.

It is evident that the particle sizes of the 1% Alg sample are in the range between 900 and 1200 nm, which is typical for dehydrated particles that maintain a spherical shape, as can be seen in Figure 5.8 (a). Regarding the incorporation of ZnO into the alginate (Alg) matrix, this is evident in Figures 5.8 (b, c, d). The white ZnO particles are uniformly distributed in the alginate mass and have sizes in the range of 20 - 50 nm. We observe that in the case of the Alg sample, the microspheres are distinctly outlined, do not show aggregation and have an irregular surface, characterized by a slight roughness and cracks formed in the dehydration process. These initial cracks were pores in the material, which will later retain the pollutant ion species they come into contact with. As for the Alg-ZnO-type spheres, their surface shows that they are occupied by small particles, due to the presence of ZnO in the initial solution and its tendency to incorporate into the mass of spheres formed in the 2% $CaCl_2$ solution.

V.4.2. SEM microscopy

The structural analysis of the Alg alginate sample used as a support material for the incorporation of ZnO in order to increase the stability of the material revealed a homogeneous spherical aspect, at magnifications of 80 x and 600 x respectively (figure 5.10), in which elements were identified by EDS analysis Ca, C, O and respectively Au, element present from the sample preparation stage which was covered with Au for conductivity (figure 5.11).

It is observed that the alginate spheres are of micron size, they constitute the future support for ZnO nanoparticles.

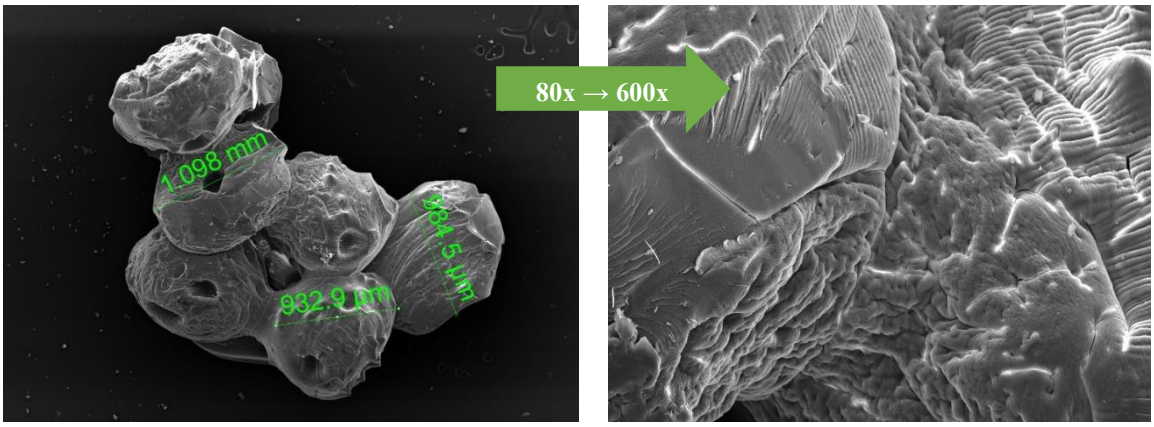

Figure 5. 10 Appearance of the 1% Alg sample at 80x and 600x magnifications.

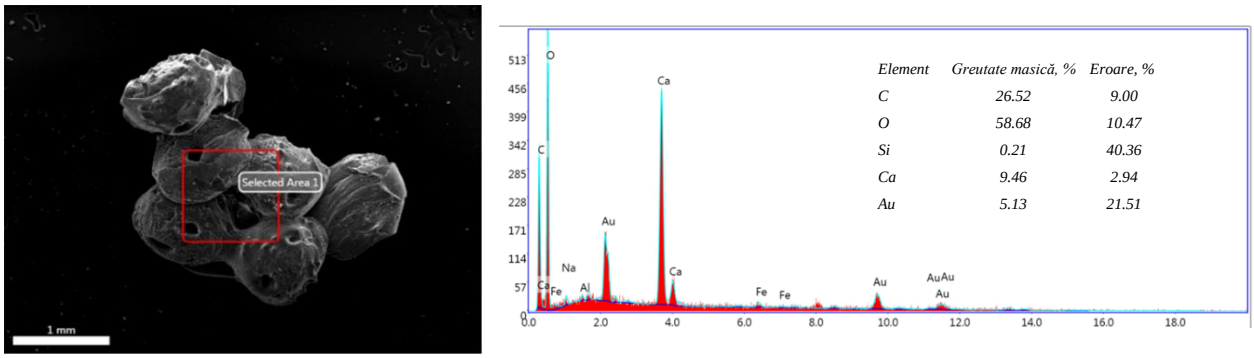

Figure 5. 11 EDS elemental analysis for the Alg 1% sample.

In the case of the Alg-ZnOg sample, the structural aspect indicates, at magnifications of 80x, 600x and 80000x, respectively, well-defined structures in which the ZnO nanoparticles are anchored in the Alg polymer matrix (figure 5.12).

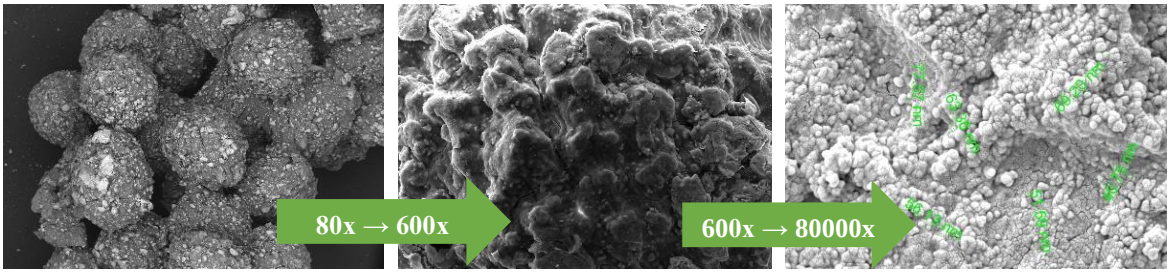

Figure 5. 12 Appearance of Alg-ZnOg sample at 80x, 600x and 80000x magnifications.

It can be seen that the dimensions of ZnOg NPs in the surface of Alg spheres have an average size of about 60 nm, which validates the dimensions obtained for ZnOg powders.

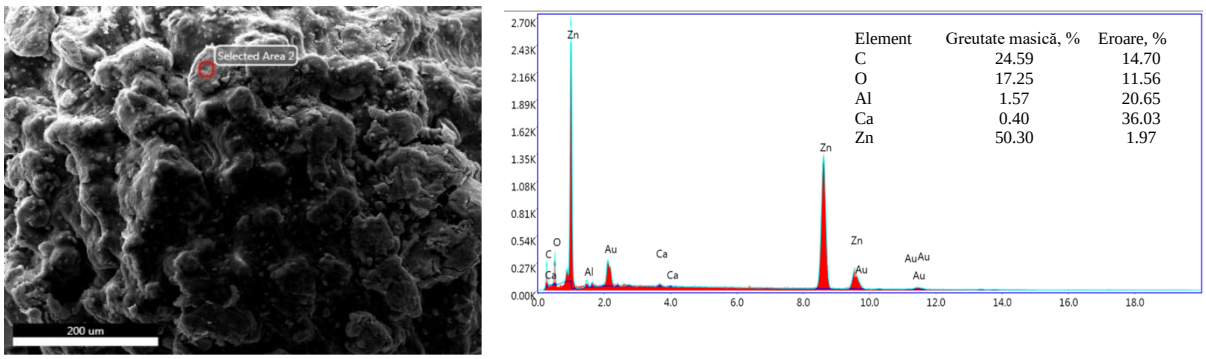

Figure 5. 13 EDS elemental analysis for the Alg-ZnOg sample.

In the case of the EDS analysis (figure 5.13), it can be seen that the presence of Zn and Ca is confirmed on the selected surface area, Al being due to alginate impurities, and Au coming from the coating process. The distribution of elements in the Alg-ZnOg sample indicates a homogeneity of the distribution of elements on the Alg surface, with a slight tendency for ZnO nanoparticles to agglomerate, as a result of their reactivity.

In the case of the Alg-ZnOp sample, the structural aspect indicates, at magnifications of 80x, 600x and 80000x, respectively, well-defined structures in which the ZnO nanoparticles are anchored in the Alg polymer matrix (figure 5.14).

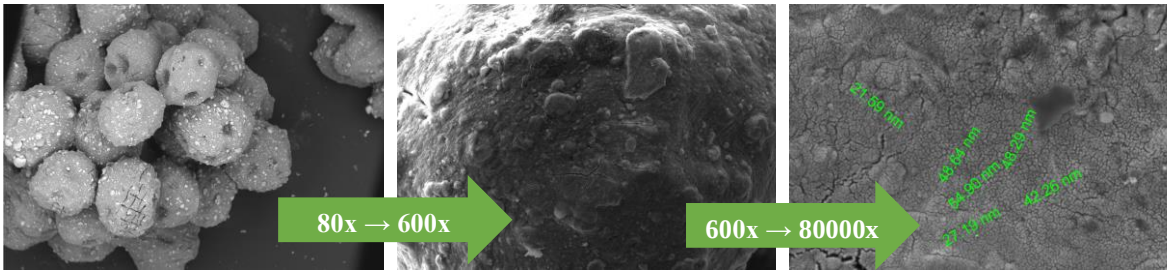

Figure 5. 14 Appearance of Alg-ZnOp sample at 80x, 600x and 80000x magnifications.

It can be seen that the dimensions of the ZnOp NPs on the surface of the Alg spheres have average dimensions of about 40 nm, which validates the dimensions obtained for the powders.

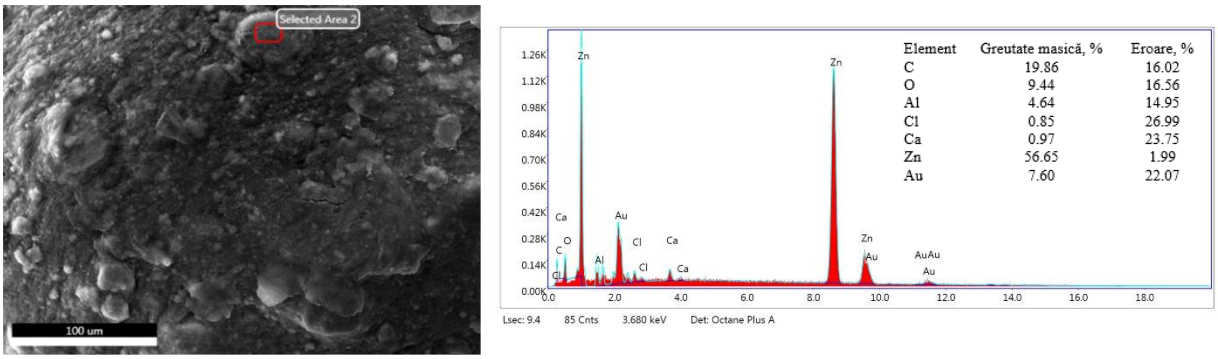

Figure 5. 15 EDS elemental analysis for the Alg-ZnOp sample.

In the case of the EDS analysis (figure 5.15), it can be seen that the presence of Zn and Ca is confirmed on the selected surface area, Al being due to alginate impurities, and Au

coming from the coating process. The distribution of elements in the Alg-ZnOp sample indicates a homogeneity of the distribution of elements on the Alg surface, with a slight tendency for ZnO nanoparticles to agglomerate, as a result of their reactivity.

In the case of the Alg-ZnOs sample, the structural aspect indicates, at magnifications of 80x, 600x and 80000x, respectively, well-defined structures in which the ZnO nanoparticles are anchored in the Alg polymer matrix (figure 5.16).

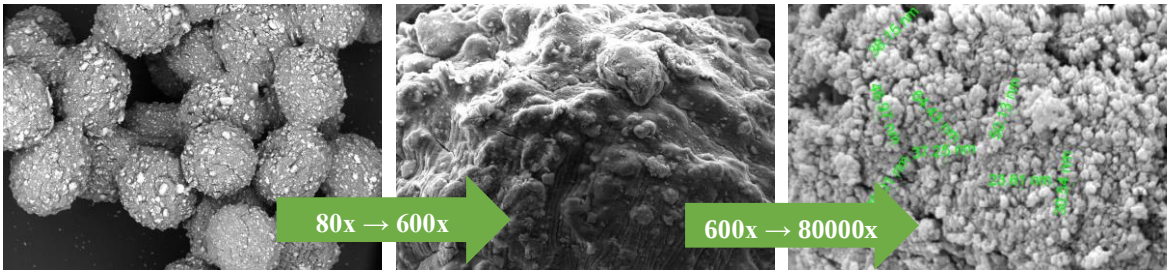

Figure 5. 16 Appearance of Alg-ZnOg sample at 80x, 600x and 80000x magnifications.

It can be seen that the dimensions of the ZnOs NPs on the surface of the Alg spheres have average dimensions of about 50 nm, which validates the dimensions obtained for the powders.

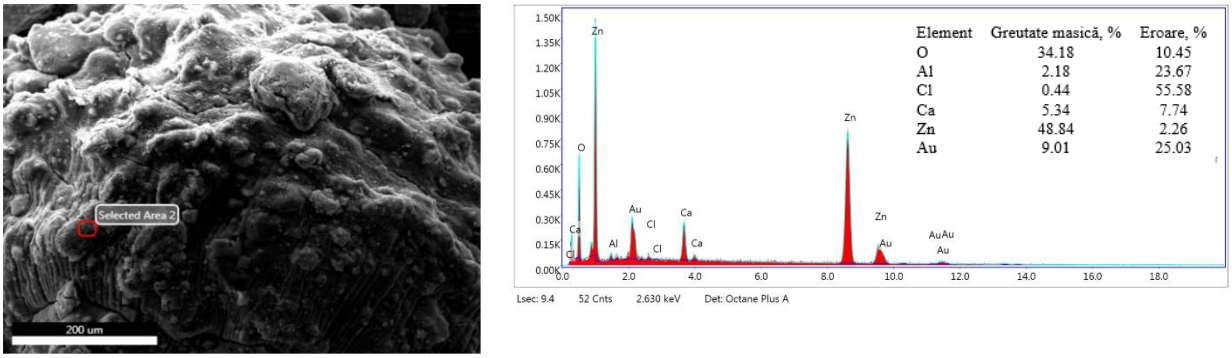

Figure 5. 17 EDS elemental analysis for the Alg-ZnOs sample.

In the case of the EDS analysis (figure 5.17), it can be seen that the presence of Zn and Ca is confirmed on the selected surface area, Al being due to alginate impurities, and Au coming from the coating process. The distribution of elements in the Alg-ZnOs sample indicates a homogeneity of the distribution of elements on the Alg surface, with a slight tendency for ZnO nanoparticles to agglomerate, as a result of their reactivity.

V.5. Partial conclusions

Following the morphological, structural and surface characterizations for the ZnO NPs eco-materials, it was found that sizes between 50 and 150 nm were obtained for the ZnO materials from grapefruit extract and ZnO synthesized by the classical method, but for the other two materials synthesized ZnO from pomelo extract and ZnO from grape extract the sizes are in the range of 100-500 nm, which means that the nanoparticles are found in distinct

agglomerates, the spherical configuration being maintained, this being a common characteristic of nanoscale particles.

The XRD analyzes also confirm the majority percentage of ZnO for the ZnOg and ZnOc samples, which is 92% and 86% ZnO respectively in the analyzed samples, whereas the ZnOp samples contain approximately 63% ZnO and ZnOs 33.6% ZnO.

Following the morphological, structural and dimensional characterizations of samples of plain Alg or with incorporated ZnO, it was found that alginate spheres tend to keep their spherical and regular shape, even if the samples contain ZnO nanoparticles or not.

CHAPTER VI. PHOTOCATALYTIC DEGRADATION TESTS

The results obtained during these experiments were based on the documentary study described in chapters I and II and were carried out during a 3-month Erasmus+ internship in the laboratory of the École Nationale Supérieure de Chimie de Rennes in France between February and April 2022.

This study was conducted to determine the ideal conditions for the decomposition of CLF in an aqueous solution, as well as to analyze the photocatalytic decomposition kinetics in the UV/ZnO system using 3 types of ZnO powders synthesized with plant extracts and 3 eco - innovative materials synthesized with the help of the 3 powders incorporated in sodium alginate matrix. The equipment presented in Chapter III was used to monitor the parameters of the photocatalytic reactions.

Water samples that have undergone photocatalytic oxide eco-materials treatment were subjected to analyzes using high performance liquid chromatography (HPLC) equipment and the SHIMADZU TOC-VCPH system.

VI.1. Photocatalytic degradation kinetics study of ZnO-based eco-materials with plant extract

VI.1.1. Photocatalytic degradation of clofibric acid using different ZnO catalysts with plant extract

In order to choose the optimal catalyst for the degradation of emergent pollutants, tests were carried out using the 3 types of ZnO with plant extract obtained according to the synthesis methods described in chapters IV.1.1., IV.1.2. and IV.1.3.: ZnOp, ZnOg, ZnOs, compared to ZnOc obtained by the classical method described in chapter IV.1.4. The emerging pollutant selected was clofibric acid (CLF) whose characteristics are presented in chapter III.5.

Tests were conducted using a concentration of 10 mg/L CLF and a concentration of 100 mg/L catalyst. Irradiation of the solution with the UV lamp was carried out for a maximum period of 6 hours at maximum intensity of irradiation and the natural pH of the solution. The tests followed the photocatalytic protocol described in chapter I.2.2. As previously explained in chapter III.7., the residual pollutant concentration and total organic carbon content were evaluated using an HPLC and TOC analyzer at different reaction times. Figure 6.1 illustrates the results obtained for the degradation (a) and mineralization (b) of clofibric acid in the presence of the evaluated catalysts.

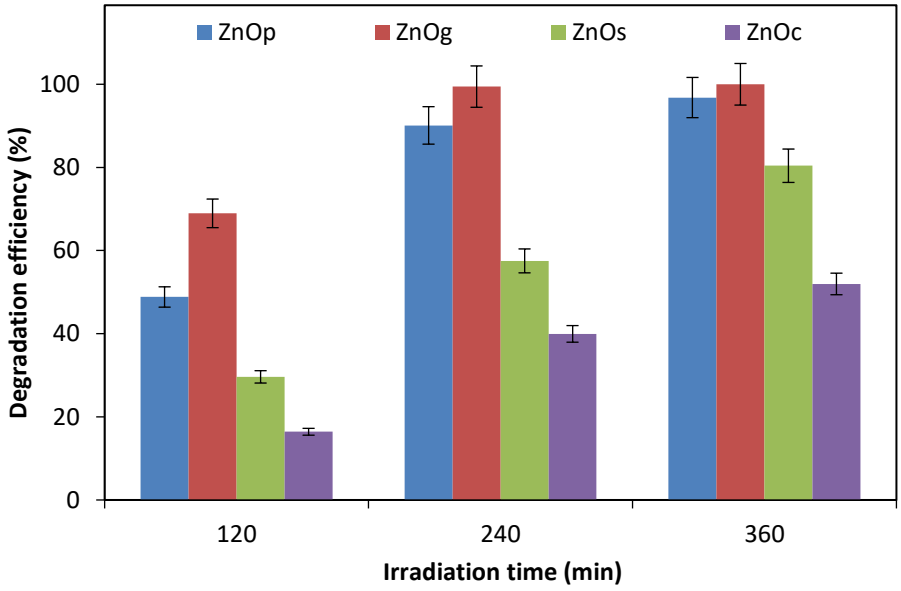

(a)

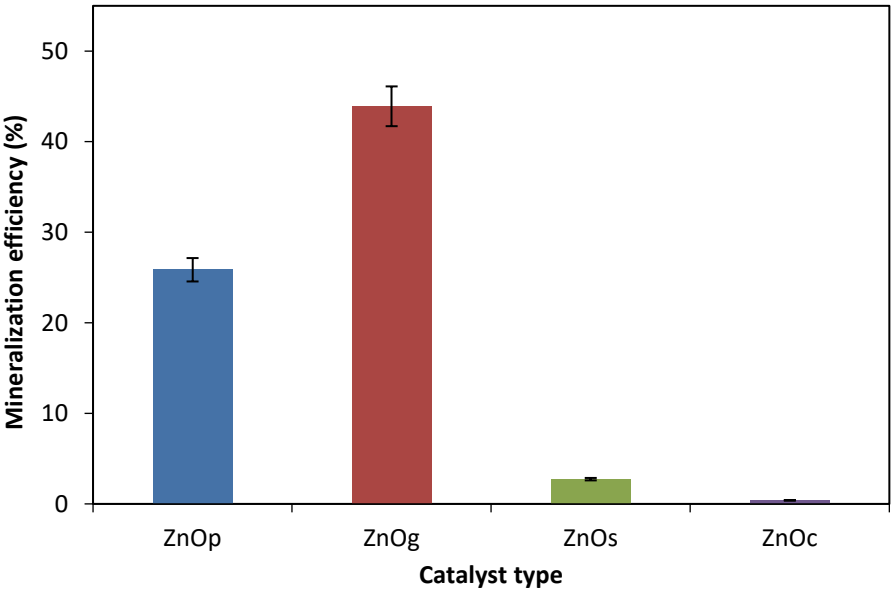

(b)

Figure 6. 1Comparison of (a) CLF photocatalytic degradation efficiency and (b) mineralization efficiency using the 4 ZnO photocatalysts.

The increased efficiency can be observed in the case of ZnO synthesized by the green method, especially in the case of ZnOg (ZnO-grapefruit). This may be because grapefruit (C. paradisi) peel extract contains a higher number of bioactive compounds namely naringin and naringenin which are flavonoids and are found only in grapefruit. Also found only in grapefruit is the related compound kaempferol, which has a hydroxyl group next to the ketone group [37]. This can be confirmed by other researchers who synthesized NP-ZnO with C. Paradisi extract [38].

After 360 minutes of irradiation, the effectiveness for ZnOg was 100%, while for ZnOp it was 96%, for ZnOs it was 80% and for ZnO it was 52%, the evolution being: ZnOg > ZnOp > ZnOs > ZnO. It is evident that the grapefruit extract improves the efficacy of the synthesized nanoparticles. This result is supported by the mineralization efficiency, which was 44% for ZnOg, while for the other 3 types of ZnO it was in the range of 1-25%.

The obtained data clearly show that ZnOg is the best catalyst to decompose CLF by exposure to UV light.

The results obtained are comparable to other studies in the literature [39].

VI.1.2. Photolytic and adsorption studies

The degradation of clofibric acid was investigated under different experimental conditions to establish the adsorption of CLF on the ZnO surface and compare direct photolysis with photocatalysis . The experimental conditions used were 10 mg/L CLF, 500 mg/L ZnOg, natural pH and maximum irradiation flux.

The tests performed represented a preliminary stage for the following experiments and kinetic interpretations in order to eliminate errors associated with non-photocatalytic damage.

The favorable impact of photocatalysis is seen in Figure 6.2, where photolysis as a single process (UV only) leads to a 25% CLF degradation after 360 minutes, but increases to 100% in the presence of the photocatalyst (ZnOg + UV). Adsorption of clofibric acid (only ZnOg) on ZnO was found to be less than 5%.

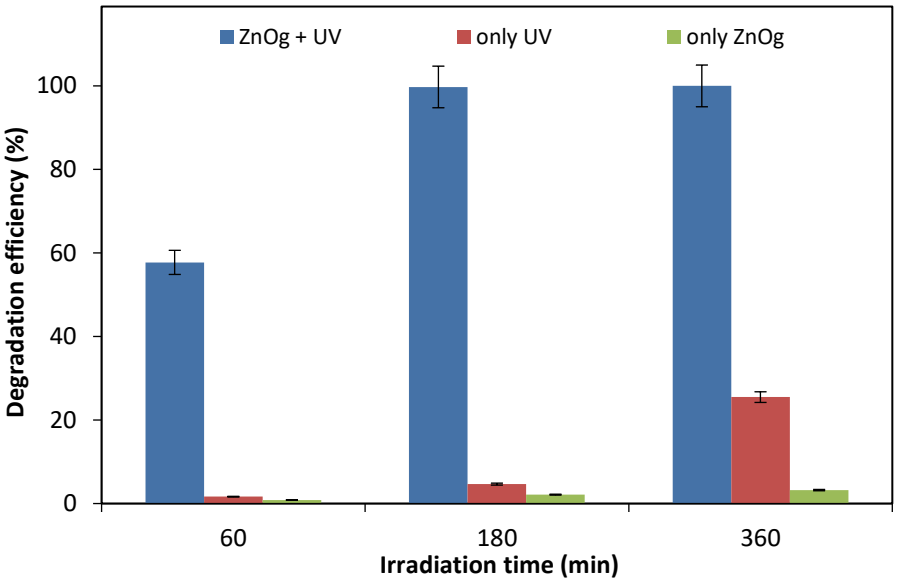

Figure 6. 2 Effect of UV light radiation and ZnO on the photocatalytic removal of CLF.

It can be concluded that the photocatalytic reaction is fully responsible for the high degradation observed in the UV/ZnO process. UV light and photocatalyst were required for efficient degradation of CLF in these tests. Photocatalysis uses the concept of light stimulation of a semiconductor. The semiconductor, or catalyst (ZnO), creates highly oxidizing free radicals in response to photons, allowing the destruction of compounds adsorbed on its surface. Active species formed during the photocatalysis process in the presence of a catalyst, such as the •OH radical, may be responsible for this behavior [40]. The photocatalytic process has active radicals such as $\bullet O^{2-}$ or •OH. There are three methods of formation of •OH radicals: (1) water and HO^- from the aqueous environment are most likely oxidized by photoinduced h^+ and produce •OH radicals; (2) O_2 in the liquid is reduced by the photoinduced electron to produce $\bullet O^{2-}$, which is then followed by the appearance of a gap (production of •OOH); (3) and subsequent reduction with production of •OH radicals. In addition, h^+ whose appearance is induced by light has proven oxidizing properties for the direct decomposition of natural contaminants, the amount of which depends on the type of catalyst and the oxidation orders [41] according to reactions 1-10 mentioned in chapter I.2.2.

Sarasidis et al. [42] obtained similar conclusions regarding diclofenac degradation in their study.

Tests were also performed on the ZnO / visible system to ensure the correct choice of working parameters in this case. The generation of •OH radicals is inhibited due to the reduced production of h + by visible light compared to UV, as seen in the following figure, where the increase in the rate of degradation using UV light at the expense of visible light is evident, but also the decrease in the rate when degradation occurs in the dark (Figure 6.3):

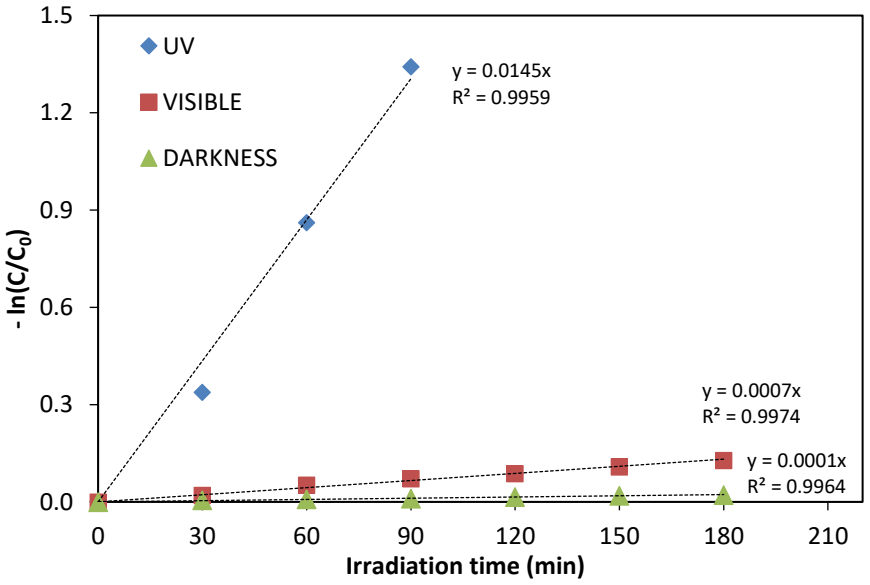

Figure 6. 3 Effect of UV light / visible light radiation and ZnOg on the photocatalytic removal of CLF.

VI.1.3. Degradation of various pharmaceutical pollutants

To confirm the effectiveness of the chosen catalyst, tests were also performed on other emergent pollutants commonly present in wastewater. Thus, in addition to clofibric acid (CLF) at a concentration of 5 mg/L , other pharmaceutical compounds were also studied such as: pentoxifylline (PTX) at a concentration of 6.5 mg/L and chloroxylenol (PCMX) at a concentration of 3.65 mg/L , but also the effect of 2 combined compounds clofibric acid and chloroxylenol (CLF + PCMX) at 5 mg/L + 3.65 mg/. The experimental conditions were the following: ZnOg = 1000 mg/L, natural pH and maximum irradiation flow.

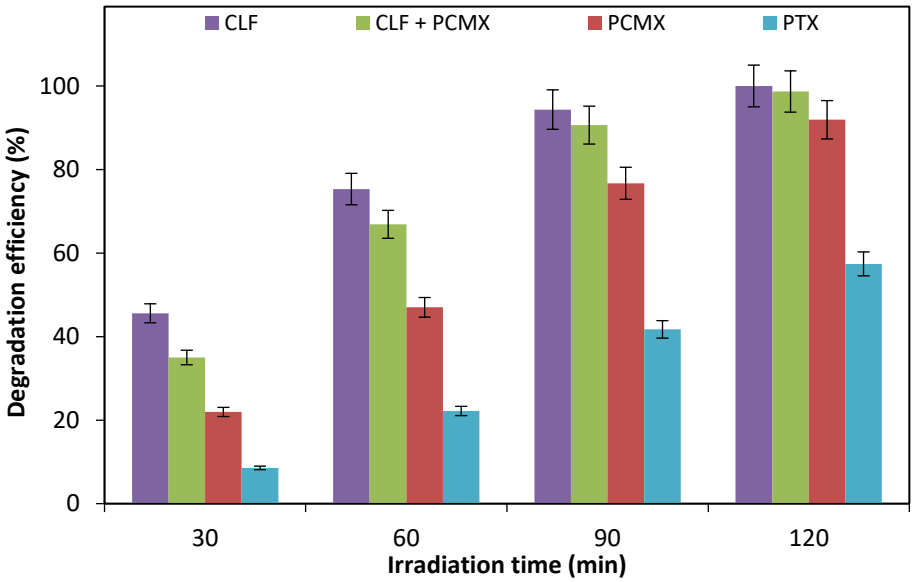

Figure 6. 4 Effect of various pharmaceutical pollutants on photodegradation efficiency.

As can be seen in Figure 6.4, the degradation efficiency is 100% after 120 minutes of irradiation for CLF, 98.67% for the combination of CLF + PCMX, 91.90% for PCMX, instead only 57.59% for PTX.

Since CLF degrades the fastest, it was selected as the target pollutant for optimization of the degradation process.

VI.1.4. Effect of catalyst concentration

ZnO has a significant impact on the degradation rate during the photodegradation process, and its concentration is one of the decisive factors in determining the efficiency. When using ZnOg, the concentration varied from 20 to 2000 mg/L, keeping the pollutant concentration constant at 10 mg/L. Experimental conditions were: natural pH and maximum irradiation flux.

From the data obtained in Figure 6.5, it can be seen that the CLF photodegradation efficiency increased with increasing ZnOg concentration from 20 to 1000 mg/L and decreased for 2000 mg/L. For a catalyst concentration of 1000 mg/L, a removal efficiency of 98% was obtained, and for 2000 mg/L, only 89% of the pollutant was removed after 120 minutes of irradiation.

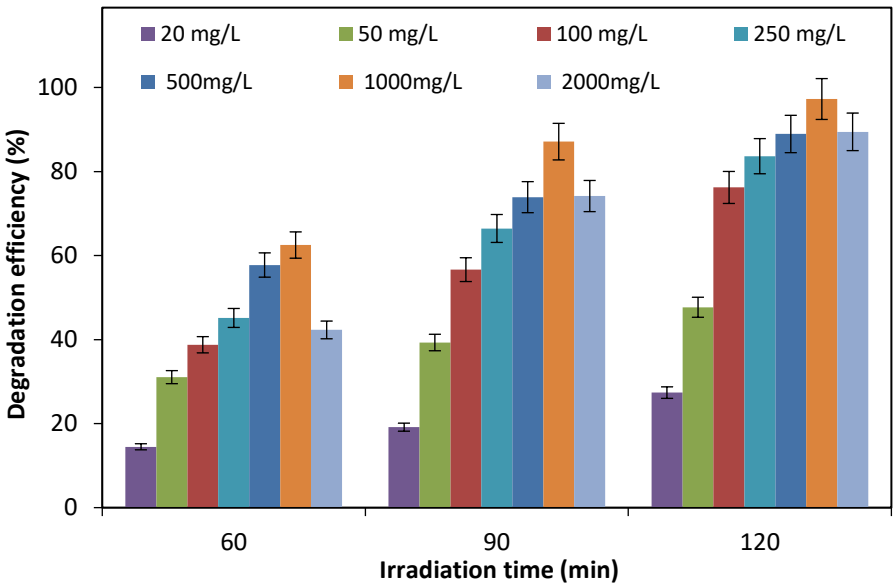

Figure 6. 5 Effect of ZnO amount on CLF photodegradation efficiency.

We can also see that the degradation rate for 2000 mg/L is lower than for 1000 mg/L. This observation can be explained by increasing the ZnO catalyst concentration above a threshold value, causing the degradation rate to decrease by increasing the turbidity of the solution and the appearance of the scattering effect. As a result, the number of active sites on the catalyst surface was limited and also UV light could not penetrate the suspension [43].

Complete photodegradation of an organic pollutant generally leads to the formation of various organic byproducts, carbon dioxide, and different inorganic anions and cations depending on the chemical structure of the target molecule. The analysis of total organic carbon (TOC) was used to determine the degree of mineralization of the pollutant following the applied treatment. The experimental data clearly showed a removal of 76 % (Figure 6.6) of total organic carbon within 6 hours of irradiation for a catalyst concentration of 1000 mg/L.

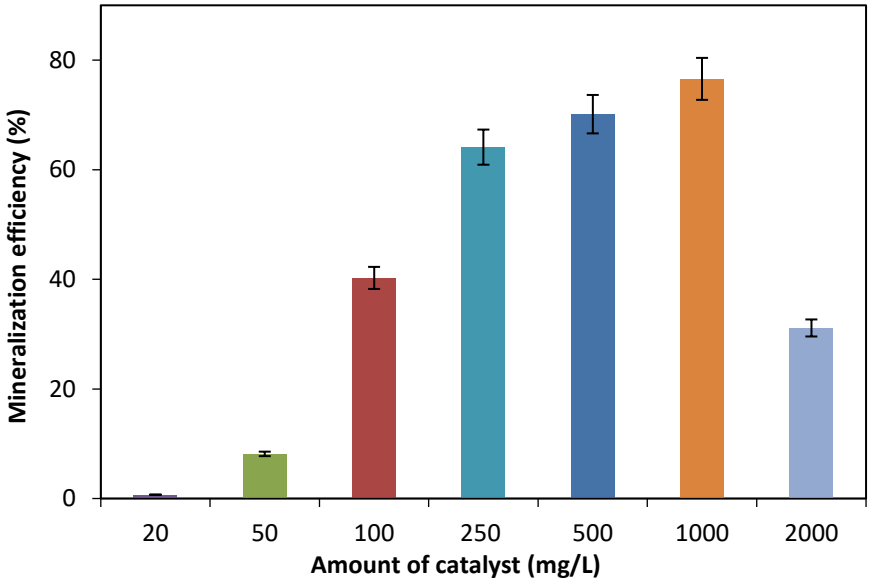

Figure 6. 6 Total organic carbon removal efficiency after 6 hours of irradiation.

It was thus observed that the efficiency of mineralization is lower than the efficiency of photocatalytic degradation due to the presence of transient organic intermediates that are formed during the photocatalytic reaction. HPLC analysis of the irradiated solutions confirms this result. Some reaction intermediates were observed during the photocatalytic reaction (Figure 6.7). This was confirmed by the response time analysis of the HPLC chromatograms as well as the results of the total organic carbon measurements. However, some observed intermediates were not subsequently mineralized at the end of the considered reaction time, but it can be assumed that by extending the irradiation time, these intermediates will be transformed into CO_2 and H_2O.

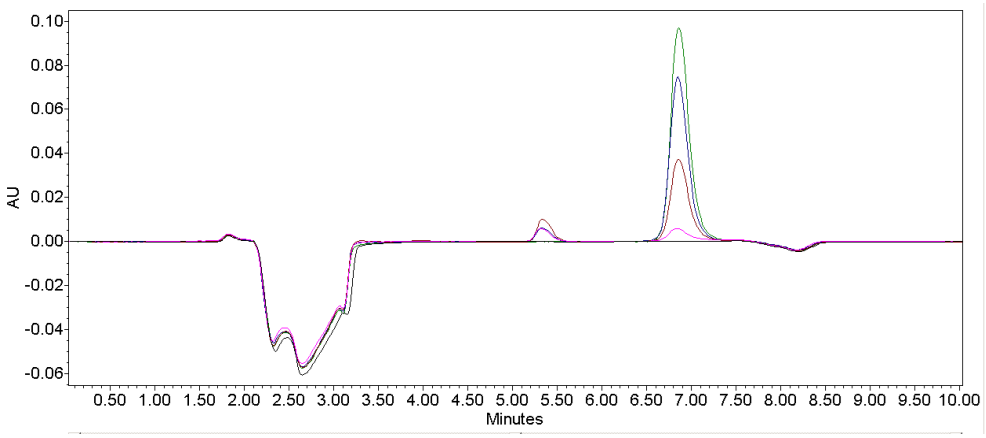

Figure 6. 7 2HPLC chromatograms obtained for an aqueous solution of 10 mg/L CLF following photocatalytic treatment with 1 g/L ZnOg and maximum irradiation flow resulting at different reaction times.

It is also important to note that the optimal value of the amount of catalyst used will be greatly influenced by the type and initial concentration of the pollutant, as well as the operating parameters of the photoreactor [44].

Other studies in the literature reported similar results for the photocatalytic degradation of catechol using ZnO nanoparticles as a catalyst [45].

The following experiments were carried out using 1 g/L ZnO, following the results presented.

VI.1.5. Effect of pollutant concentration

In real waters, various organic chemicals are present, in different amounts, thus it is necessary to investigate the influence of the initial concentration of organic pollutants on their removal efficiency. Figure 6.8 illustrates the degradation efficiency by varying the CLF concentration for 5 initial concentrations between 5 and 100 ppm, the amount of ZnO (1g/L) being constant, the maximum irradiation flux and the natural pH.

With an increase in the initial concentration of the pollutant solution from 5 to 100 mg/L, the photodegradation percentage decreased from 100% to 60% after an irradiation period of 120 minutes, according to the data shown in Figure 6.8. Also, the mineralization efficiency is shown in figure 6.9, where the degradation results can be confirmed and it can be seen how the mineralization decreases from 87% to 55% with increasing pollutant concentration.

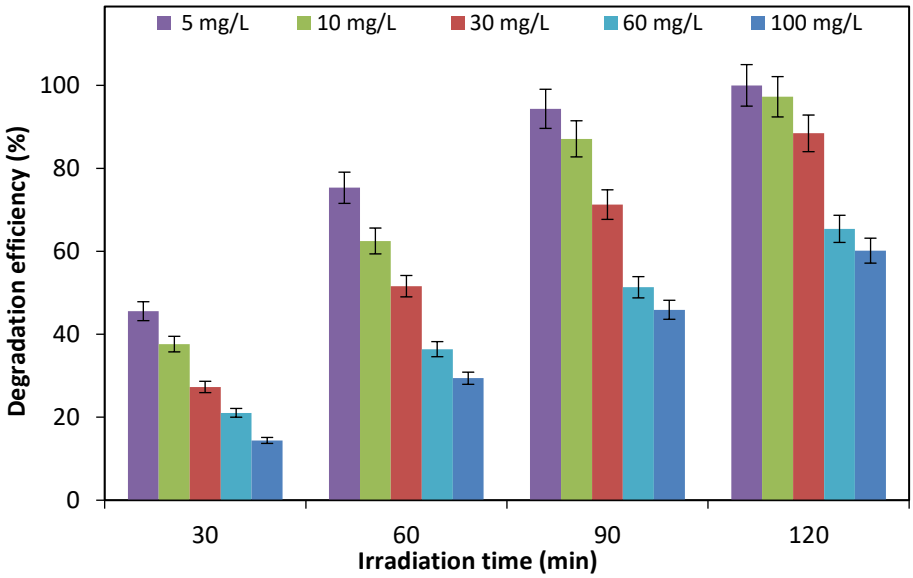

Figure 6. 8 Effect of initial amount of CLF on degradation efficiency.

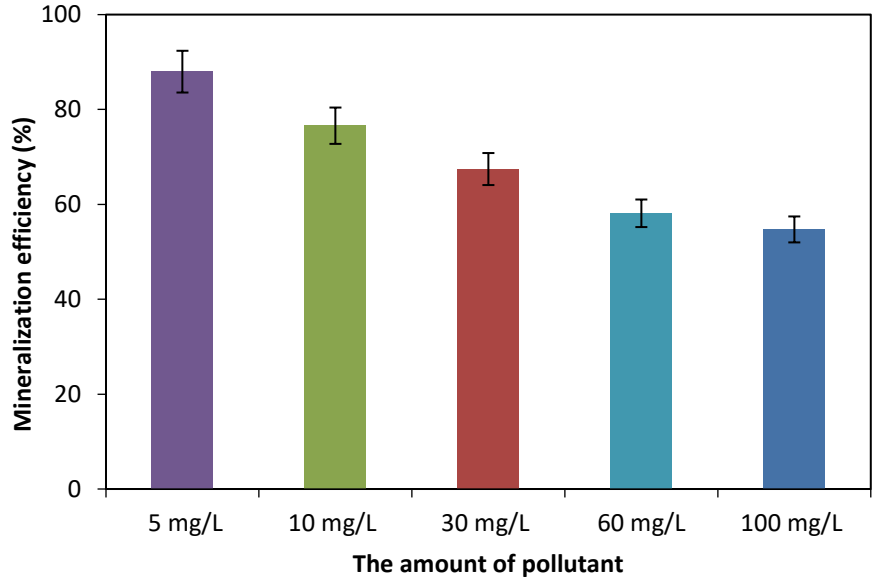

Figure 6. 9 3Effect of the initial amount of CLF on the mineralization efficiency after an irradiation time of 360 minutes.

The observed effect can be attributed to a decrease in the number of active sites on the catalyst surface, which is proportional to the initial CLF concentration. As a consequence, the rate of formation of hydroxyl radicals on the catalyst surface will decrease. This kinetic behavior is common in photocatalytic systems, as other researchers have obtained similar results for the photocatalytic oxidation of other contaminants [46].

Considering the results obtained, a quantity of 5 mg/L CLF will be used for the following photodegradation tests.

VI.1.6. Effect of light intensity

One of the elements influencing the photocatalytic process on organic substrates is the light intensity. A relatively high intensity of UV light is required to provide enough photon energy on the active surface of ZnO to achieve a high photocatalytic reaction rate, especially in water treatment.

The effect of light intensity on degradation and mineralization efficiency was examined at a constant pollutant concentration (5 mg/L) and a constant catalyst loading (1 g/L). The experimental conditions of the UV lamp are the following: UVmin = 0.07 mW/cm^2, UVmed = 1.56 mW/cm^2, UVmax = 5.56 mW/cm^2 .

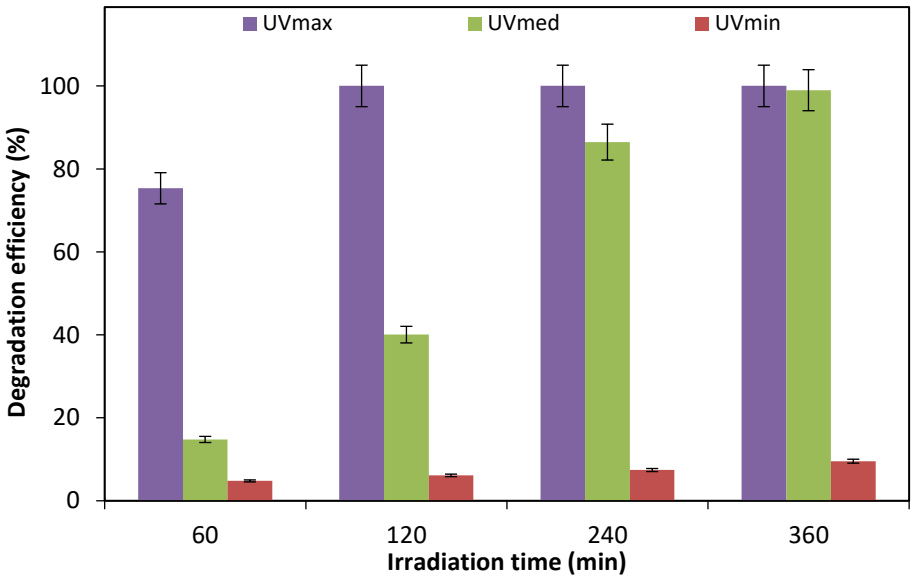

(a)

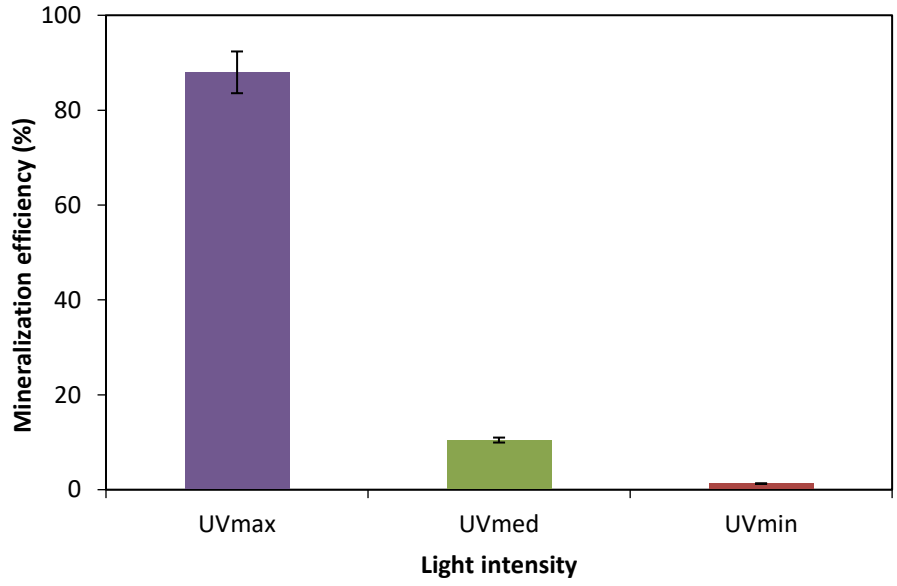

(b)

Figure 6. 40 Effect of light intensity on (a) CLF degradation efficiency and (b) its mineralization after 360 min of irradiation.

According to the data shown in Figure 6.10 (a, b), the percentage of photodegradation and mineralization of CLF increased as the light intensity increased.

It was observed that the percentage of CLF decomposed after 120 minutes of irradiation increased from 6% at the lowest light intensity (0.07 mW/cm^2), reached 40% at an average light intensity (1.56 mW/cm^2) and reached 100% at the highest light intensity (5.56 mW/cm^2). It can be seen that after a long time (360 min) of irradiation with medium light, the degradation of the compound can reach almost 100%, but the mineralization decreases from 87% (UVmax) to 10% (UVmed) and respectively less than 5 % (UVmin). As a result, it is preferable that the UV lamp is used to its full potential. Radiant light intensity was measured with a 3W VLX radiometer.

As a result, the production rate of photoactive species (electron–hole pairs) on the semiconductor particles increases, as does the rate of CLF photocatalytic degradation, as light intensity influences the wavelength and overall energy supply of a photocatalytic process.

Other studies that investigated the influence of light intensity on the photocatalytic degradation of other organic pollutants showed similar results [47].

VI.1.7. Degradation of the target compound under real conditions

Additional tests were performed in real water matrices such as bottled water (VOLVIC), tap water (TAP), well water (WELL) and well water diluted with ultrapure water (50% WELL + 50 % UPW). The results obtained were compared with those performed in ultrapure water (UPW) (figure 6.11). These tests were performed at a pollutant concentration of 5 mg/L, and a catalyst concentration of 1 g/L, natural pH, and maximum irradiation flux.

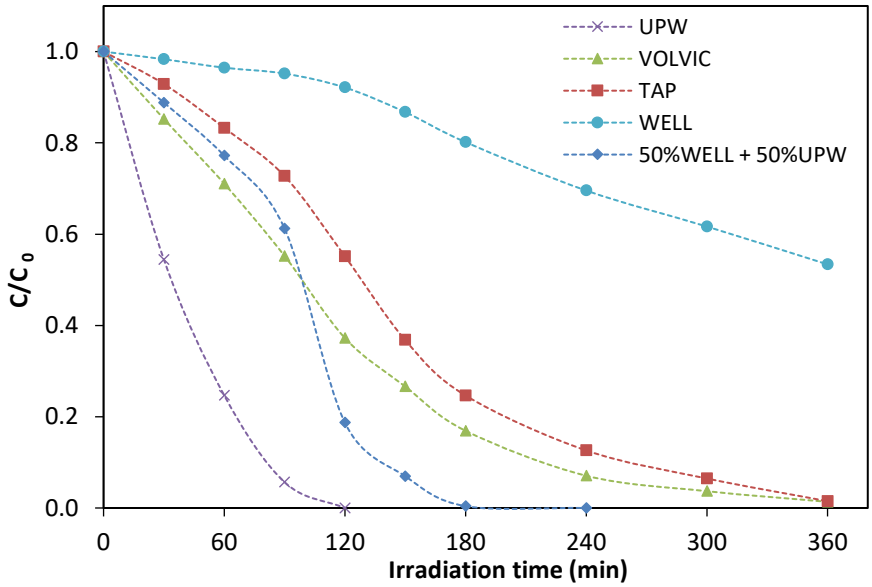

Figure 6. 11 Effect of water matrices on target compound degradation .

The obtained results confirm other studies that indicated a reduction of the photocatalytic activity depending on the complexity of the water matrix. The obtained results could be attributed to the existence of naturally occurring organic matter (NOM), which act as inhibitors of hydroxyl radicals, directly influencing the photocatalytic efficiency.

The same trend seems to have the mineralization efficiency of the compound as can be seen in figure 6.12.

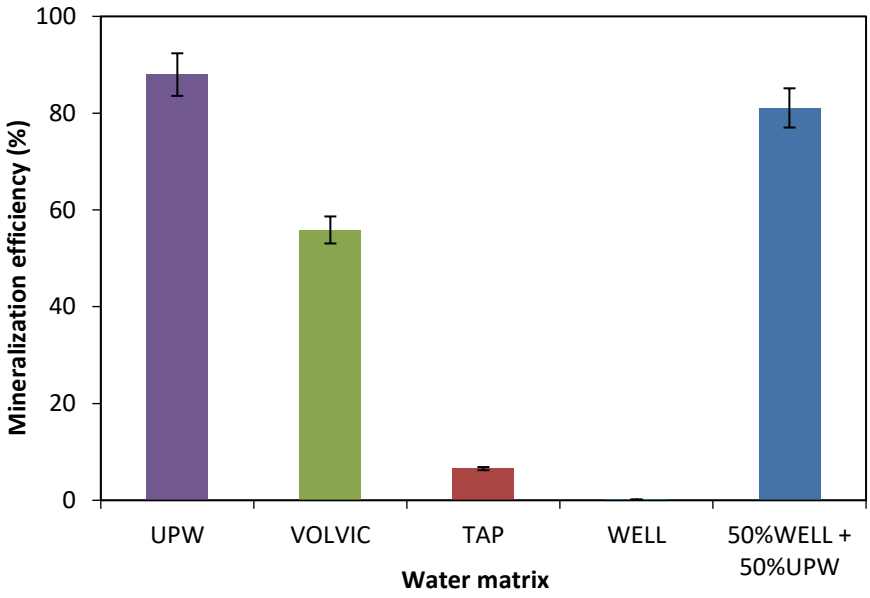

Figure 6. 5Effect of water matrix on mineralization efficiency after an irradiation time of 360 minutes.

Choi et al. [48] observed similar results when they investigated the photodegradation of SMX under UVA radiation using titanium as a photocatalyst; reported an approximately 10.5-fold decrease in rate between tests performed in ultrapure water and secondary effluent. Most of the time, this harmful effect is attributed to the presence of other organic molecules and inorganic ions, which compete with pollutants for both oxidants and active sites on the catalyst [49].

VI.1.8. Reuse

In general, several cycles can be performed using the same material and achieving nearly the same pollutant degradation efficiency. However, after a critical number of recycling cycles, the ZnO nanophotocatalyst usually shows a slight decrease in its activity [50].

Figure 6.13 demonstrates that ZnO photocatalysts can be used for up to 5 cycles without losing much of their activity, indicating that they are chemically stable under neutral conditions and that photocorrosion of ZnO is low. The experimental conditions are: CLF = 5 mg/L, ZnOg = 1 g/L, natural pH, natural pH and maximum irradiation flux.

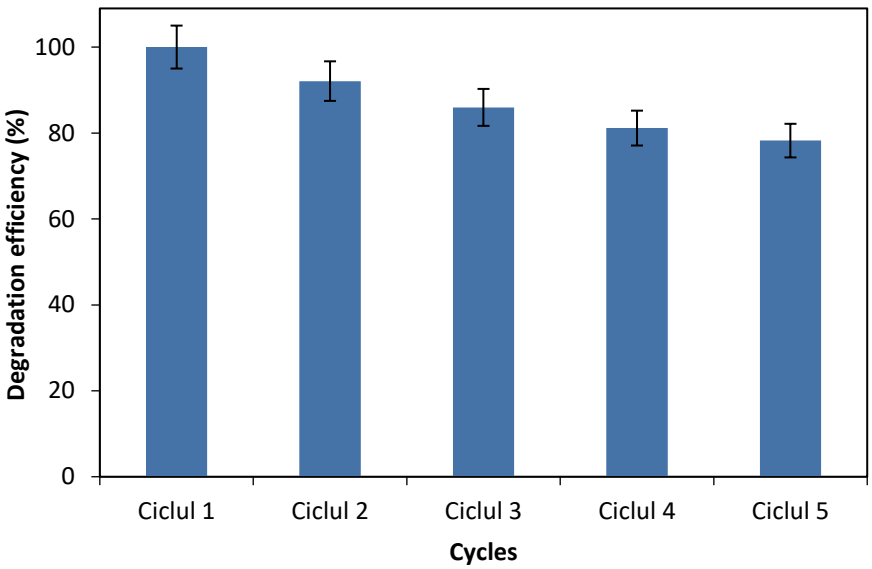

Figure 6. 13 ZnO efficiency after 5 reuse cycles at 120 minutes of irradiation.

The experiments included 5 cycles, after which the nanophotocatalyst decreased from 100% for the 1st cycle to 80% for the 5th cycle in efficiency. This performance loss can be explained by the fact that material recovery is not always complete and material losses may occur during the recovery phase when using this methodology. This would imply a lower dose on the next cycle and therefore a lower performance.

It can be seen that the reaction between the positively charged vacancies and the surface oxygen of ZnO is the key feature for the dissolution of ZnO. In addition, the vacancies on the ZnO surface also lead to photocorrosion of ZnO [51]. Some studies have reported that the photocatalytic activity of ZnO can be used up to several cycles without any loss of activity [52].

VI.2. Photocatalytic degradation kinetics study of alginate and ZnO-based eco-materials with plant extract

VI.2.1. Photocatalytic degradation of clofibric acid using different photocatalysts

Considering the performance of ZnONPs synthesized with grapefruit extract, the effectiveness that this material can have, in the case of incorporation into alginate spheres (Alg-ZnOg), was studied in order to reduce the risk of material loss. The experiments were carried out using a concentration of 10 mg/L CLF and a catalyst concentration of 500 mg/L, and the UV lamp irradiation was maximum for six hours. The tests followed the photocatalytic protocol previously described in chapter I.2.2 . As previously explained, the residual pollutant concentration was evaluated using an HPLC at different reaction times.

Figure 6.14 illustrates the results obtained for the degradation of CLF in the presence of the evaluated catalysts, ZnOg and Alg-ZnOg.

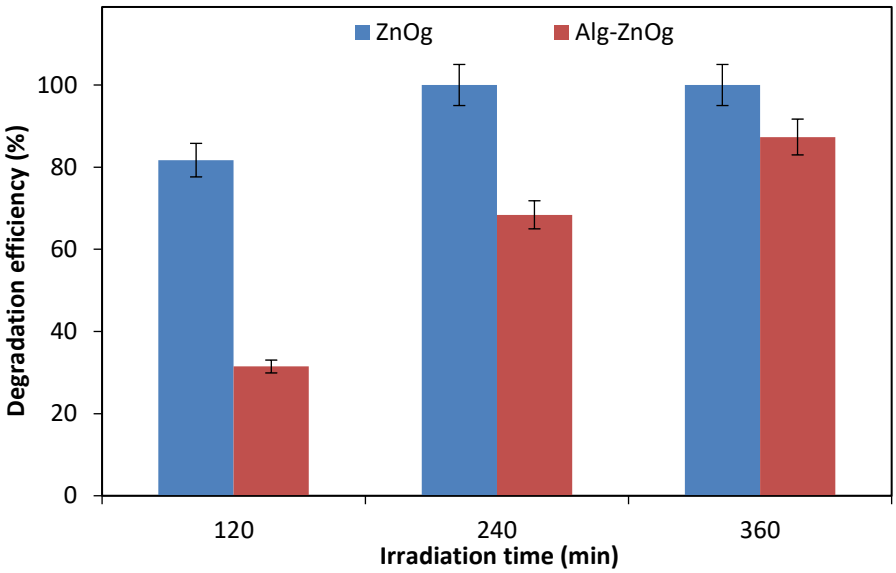

Figure 6. 14 Comparison of photocatalytic degradation efficiency of CLF using ZnOg and Alg-ZnOg.

It is evident that the Alg-ZnOg spheres have an efficiency close to that of the simple ZnOg catalyst, the differences not being significant. After 360 min of irradiation, the removal efficiency for ZnOg was 100%, while for Alg-ZnOg it was 87%. It is evident that the powder contributes to a high efficiency in the degradation of the target pollutant, through the structure and nanosized size of the particles. However, considering that an easy recovery from the aqueous environment is preferable, especially taking into account the nanometric dimensions of ZnOg that can also affect the environment through uncontrolled discharge, the Alg-ZnOg type catalyst will be analyzed in the following studies of degradation. Thus, for the following studies, Alg-ZnOg spheres were used to be tested under different conditions.

VI.2.2. Photolytic and adsorption studies

The degradation of CLF was investigated under different experimental conditions to investigate the adsorption process of CLF on the Alg-ZnOg surface and compare direct photolysis with photocatalysis. The experimental conditions are: CLF = 10 mg/L, Alg-ZnOg = 500 mg/L, natural pH and maximum irradiation flux.

These tests were necessary to eliminate errors associated with non-photocatalytic damage. It should be noted that the initial solutions were magnetically stirred in the dark for 1 h before irradiation to achieve adsorption equilibrium.

The favorable impact of photocatalysis is seen in Figure 6.15, where the photolysis process alone (UV only) results in a 25% CLF degradation after 360 minutes, but increases

to 87% in the presence of the photocatalyst (Alg-ZnOg + UV). CLF adsorption, using only Alg-ZnOg, was found to be less than 5%.

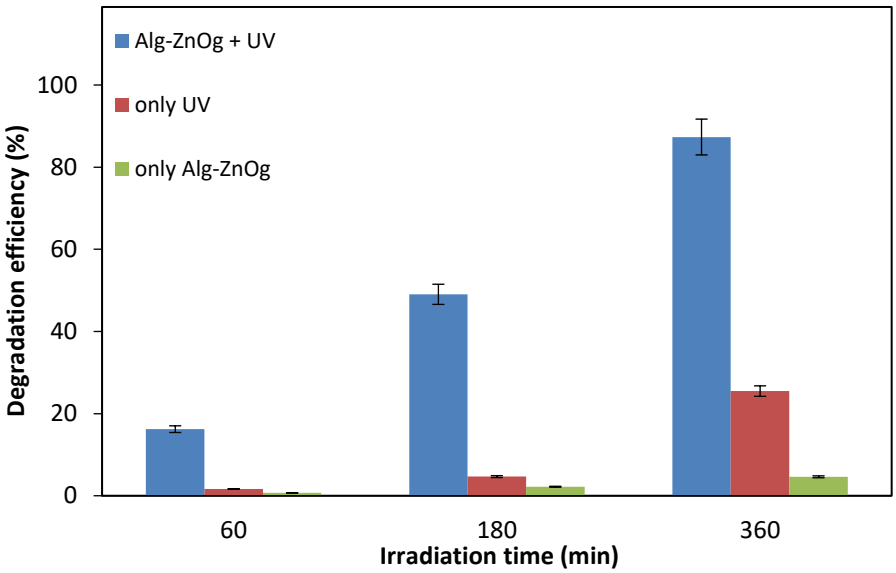

Figure 6. 15 Effect of UV light and Alg-ZnOg on the degradation efficiency of CLF.

In fact, the photocatalytic reaction is fully responsible for the high degradation observed in the UV/ZnO process. UV light and a photocatalyst such as Alg-ZnOg were required for efficient degradation of CLF in these tests.

VI.2.3. Degradation of various pollutants

To confirm the effectiveness of the chosen catalyst, numerous tests were performed on several pollutants commonly found in wastewater, such as clofibric acid (CLF), pentoxifylline (PTX) and chloroxylenol (PCMX), but also the combined effect of two of these compounds (CLF + PCMX). Experimental conditions are: CLF = 5 mg/L, CLF + PCMX = 5 mg/L + 3.65 mg/L, PCMX = 3.65 mg/L, PTX = 6.5 mg/L, Alg-ZnOg = 500 mg/L, natural pH and maximum flux irradiance.

As can be seen in Figure 6.16, the degradation efficiency is 92% after 360 minutes of irradiation for CLF, 80% for the combination of CLF + PCMX, 59% for PCMX, instead only 38% for PTX.

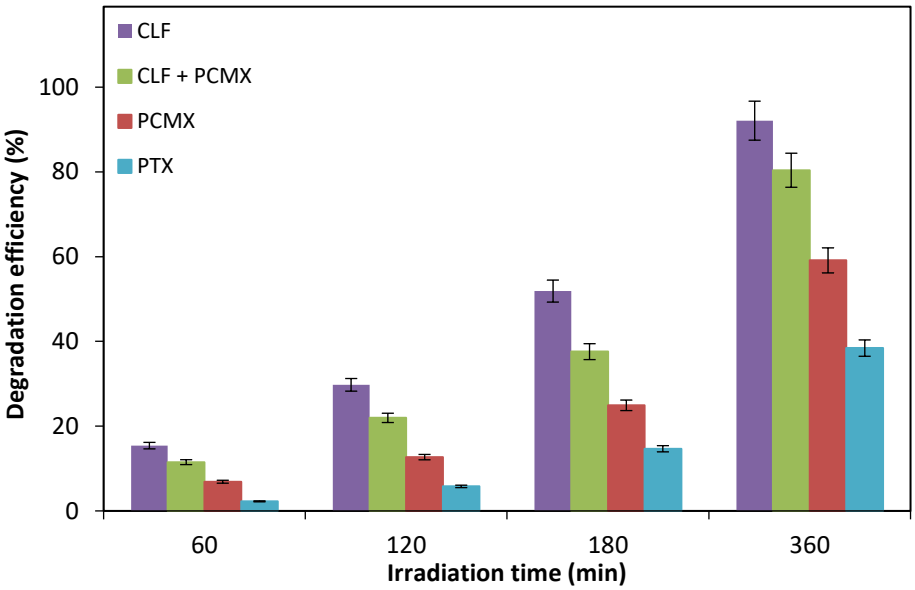

Figure 6. 16 6Effect of various pollutants on photodegradation efficiency.

The degradation efficiency is lower for some of them because they have a more complex structure and are more difficult to eliminate in a short irradiation time. Since CLF degrades the fastest, it will be the target pollutant for process optimization.

VI.2.4. Effect of catalyst dose

The initial concentration of ZnO was increased from 100 to 1000 mg/L, keeping the pollutant concentration constant at 10 ppm. Experimental conditions: CLF = 10 mg/L, Alg-ZnOg = 100, 200, 500, 1000 mg/L, natural pH and maximum irradiation flux. It can be seen from the data obtained in Figure 6.17 that the CLF removal increased as the concentration of Alg-ZnOg increased from 100 to 1000 mg/L. For a catalyst concentration of 1000 mg/L, a good removal efficiency of 87% was obtained after 360 minutes of irradiation.

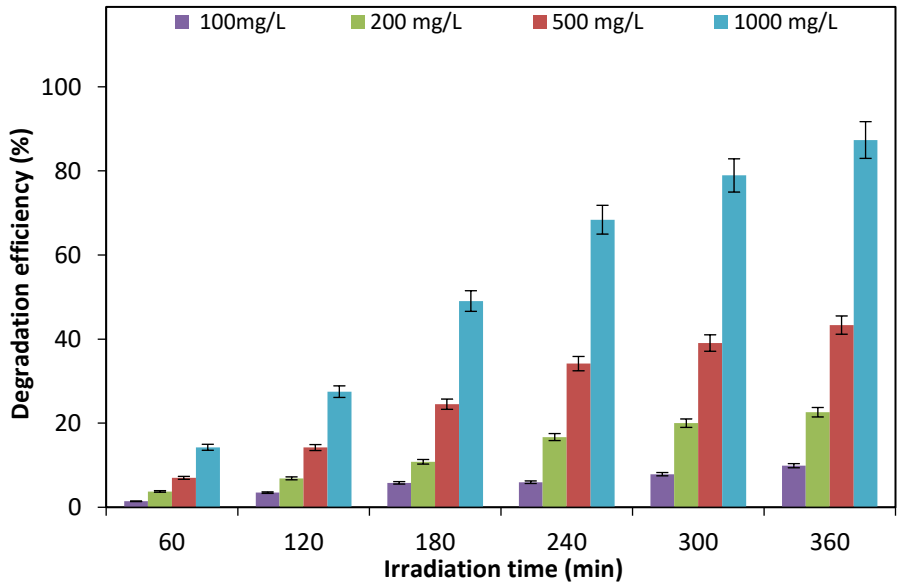

Figure 6. 17 Effect of Alg-ZnOg amount on CLF photodegradation efficiency.

It is important to emphasize that the type and initial concentration of the pollutant, together with the operating conditions of the photoreactor, will significantly influence the optimum value of the amount of catalyst added . Other studies reported similar results for photocatalytic degradation using Alg-ZnO nanoparticles as catalyst [53].

The following experiments will be performed using 1 g/L Alg-ZnOg to optimize the procedure, taking these results into account.

VI.2.5. The pollutant concentration effect

Numerous organic compounds were identified in environmental samples in different concentrations. Therefore, it is crucial to analyze how the initial concentration of organic pollution affects its removal. Figure 6.18. illustrates the degradation efficiency by varying the initial pollutant concentration from 5 to 60 ppm and keeping the amount of Alg-ZnOg (1g/L), maximum irradiation flux, and natural pH constant.

According to the results, it was observed that the percentage of photodegradation decreased from 92% to 20% after an irradiation time of 360 minutes. This decrease in photodegradation efficiency occurred as the initial pollutant solution concentration increased from 5 to 60 mg/L. Also, the efficiency of mineralization is shown in figure 6.19, where the degradation results can be confirmed and it can be seen how mineralization decreases from 15% to 1% with increasing pollutant concentration.

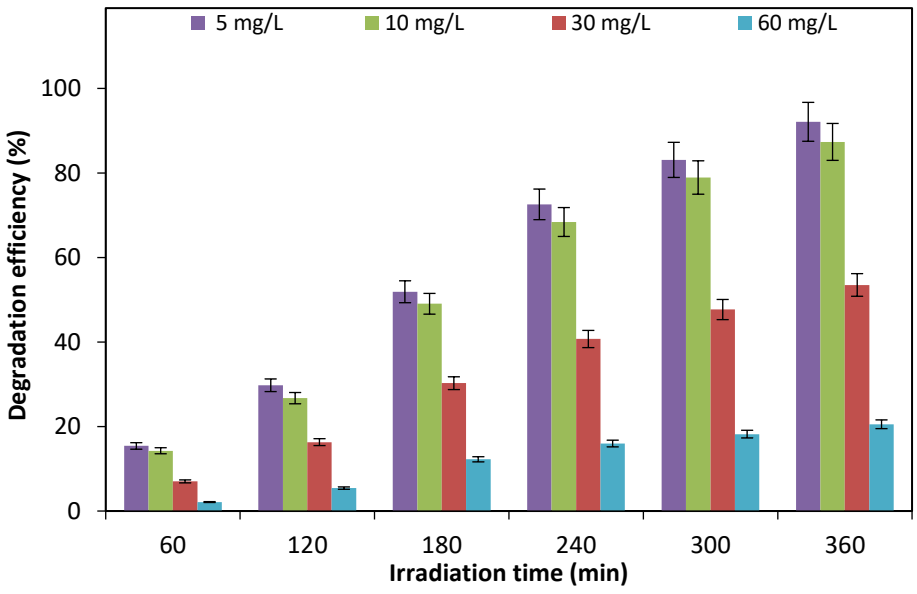

Figure 6. 18 Effect of amount of CLF on photodegradation efficiency .

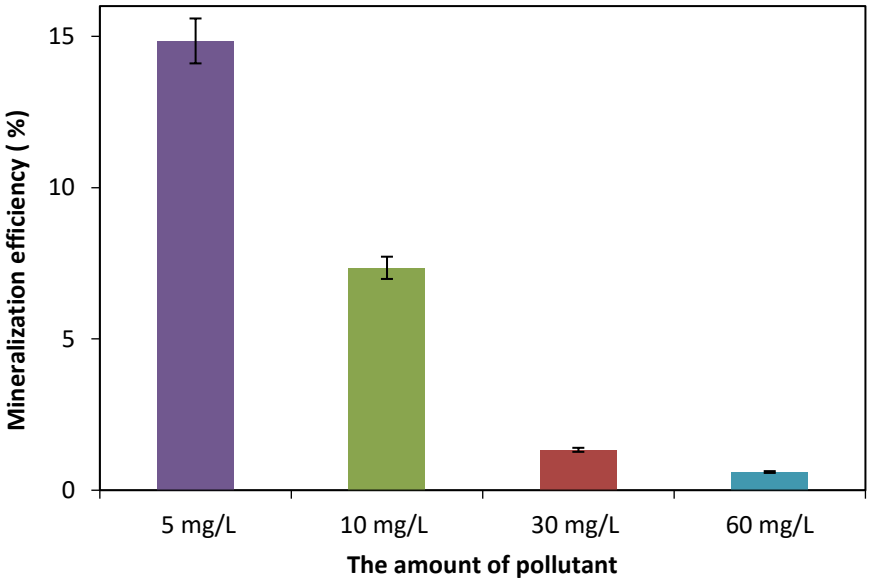

Figure 6. 19 7Effect of the initial amount of CLF on the mineralization efficiency after an irradiation time of 360 minutes.

The reduction in the number of active sites on the catalyst surface, which is proportional to the initial concentration of CLF, is the cause of the observed impact [54].

VI.2.6. Effect of UV light intensity

To ensure the efficient delivery of sufficient photon energy on the active surface of ZnO and to achieve a high photocatalytic reaction rate, especially in water treatment, it is essential to use a significant intensity of UV light. With a constant pollutant content of 5 mg/L and a constant catalyst loading of 1 g/L, the impact of light intensity on degradation and mineralization efficiency was examined. The proportion of CLF photodegradation and mineralization increased with increasing light intensity, as shown in Figure 6.20. (a, b). The experimental conditions are: natural pH, UVmin = 0.07 mW/cm^2 , UVmed = 1.56 mW/cm^2 , UVmax = 5.56mW/cm^2 . It was observed that the percentage of CLF degraded after an irradiation time of 360 minutes increased from 7% at the minimum light intensity (0.07 mW/cm^2) to 16% at the average light intensity (1.56 mW/cm^2) to 92% at maximum light intensity (5.56mW/cm^2). Mineralization was not so satisfactory even after 360 minutes, as it decreased from 15% (UVmax) to 8% (UVmed) to less than 5% (UVmin). As a result, it is preferable to use the UV lamp to its full potential. Radiant light intensity was measured with a 3W VLX radiometer. Since light intensity affects the wavelength and total energy supply of a photocatalytic process, it leads to an increase in the rate of generation of photoactive species (electron-hole pairs) on the semiconductor particles, as well as the rate of photocatalytic degradation of CLF.

.

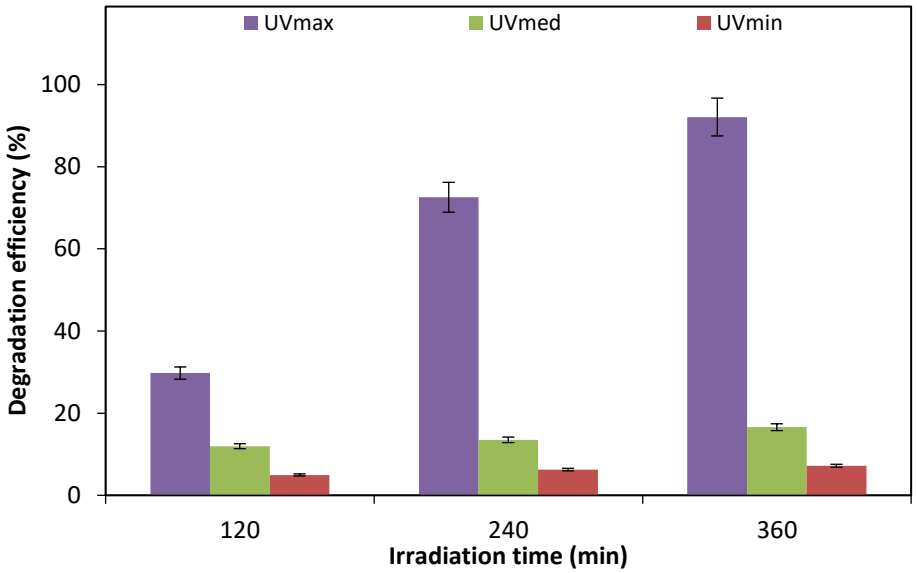

(a)

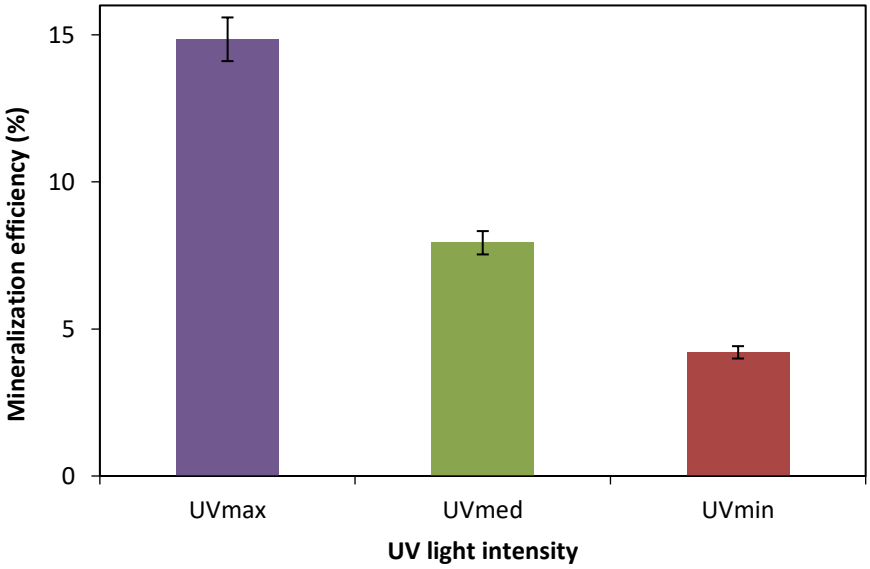

(b)

Figure 6. 20 8Effect of light intensity on (a) pollutant degradation efficiency and (b) their mineralization after 360 minutes .

VI.2.7. Degradation of the target compound under real conditions

Additional tests were performed in real water matrices such as bottled water (VOLVIC), tap water (TAP), well water (WELL) and well water diluted with ultrapure water (50% WELL + 50% UPW). With these data, findings obtained in ultrapure water were also reported for comparison purposes (figure 6.21). These tests were performed at a pollutant concentration of 5 mg/L, a catalyst concentration of 1 g/L, natural pH, and maximum irradiation flux.

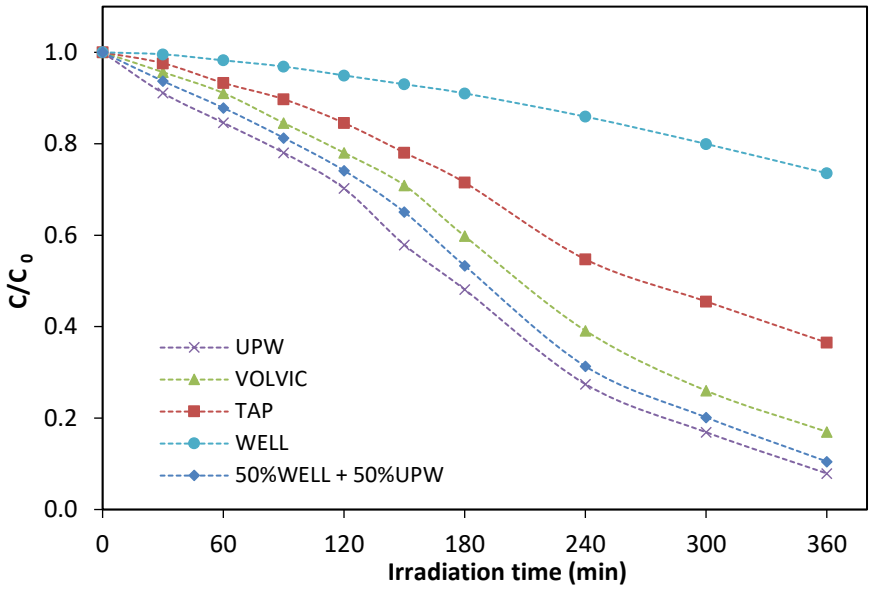

Figure 6. 91 Effect of water matrix on photodegradation efficiency.

There are numerous studies that have identified a reduction in photocatalytic activity depending on the complexity of the water matrix. These results can be explained by the presence of natural organic matter (NOM), which act as inhibitors of hydroxyl radicals and influence the effectiveness of the photocatalytic process.

VI.2.8. Reuse

In general, after several cycles of use of the same material, contaminants can be degraded with approximately the same efficiency. However, the literature indicates that the Alg-ZnO catalyst shows a slight decrease in its activity after a number of recycling steps [55].

Figure 6.22 shows that the Alg-ZnOg photocatalyst can be used up to 5 times before significantly losing its activity, thus demonstrating the chemical stability under neutral conditions and that there is no risk of photocorrosion of Alg-ZnOg. Experimental conditions: CLF = 10 mg/L, Alg-ZnOg = 1 g/L, natural pH, natural pH and maximum irradiation flux.

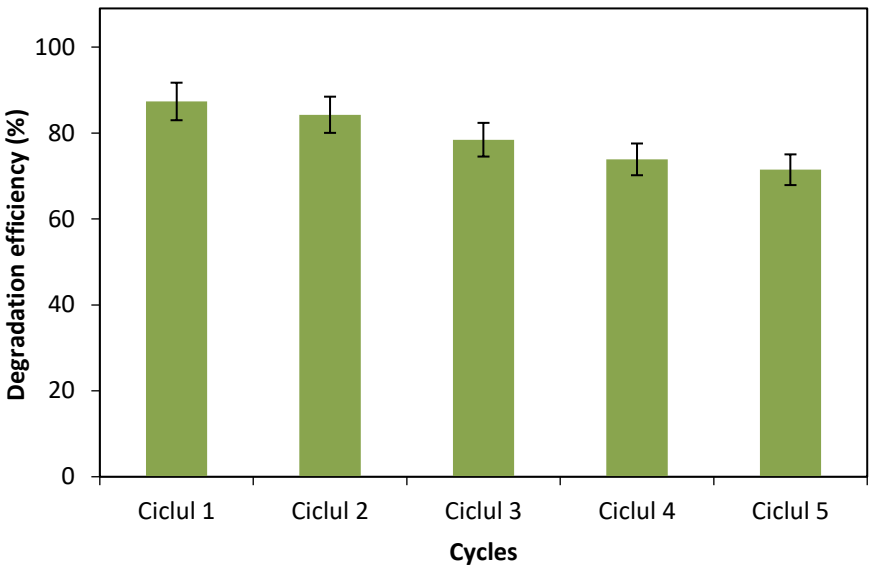

Figure 6. 22 Efficiency of Alg-ZnOg after 5 reuse cycles at 360 minutes of irradiation.

In this study, the reuse of the nanophotocatalyst was performed for 5 cycles. After the 5 reuse steps, the catalyst efficiency dropped from 87% for the first cycle to 71% for the 5th cycle.

Some previous studies reported that the photocatalytic activity of Alg-ZnO can be used numerous cycles without any loss of activity [56].

VI.3. Partial conclusions

By selecting the optimal operating conditions, an almost complete elimination of the target molecule was achieved in a time interval of about 2 hours, using a maximum irradiation intensity of 5.56 mW/cm 2 , a concentration of 5 mg/ ^{L} for pollutant and 1000 mg/L for ZnOg.

The synthesized Alg-ZnOg eco-material demonstrates significant potential in the field of environmental protection. Test results show that this material has a strong photocatalytic degradation capacity for organic compounds present in wastewater, with a removal efficiency of 92% in the UV-A range. An additional benefit of this material is that, being an immobilized catalyst, the additional step of recovering the particles from the suspension after the experiment is completed is no longer necessary.

These results suggest that the synthesized ZnOg and Alg-ZnOg eco-materials can be effectively used for the degradation of organic compounds present in waters. This has significant potential in wastewater treatment and purification, contributing to environmental protection and reducing the impact of organic pollution in aquatic ecosystems.

CHAPTER VI I. GENERAL CONCLUSIONS, PERSONAL CONTRIBUTIONS AND FUTURE RESEARCH DIRECTIONS

VII.1. General conclusions

One of the most commonly used semiconductors in photocatalysis processes is zinc oxide (ZnO), often in the form of nanoparticles. ZnO has significant photocatalytic activity and exhibits numerous advantages such as low toxicity, chemical stability, and affordable cost, making it an attractive choice for use in various environmental and water-related applications.

The effective use of ZnO in photocatalysis processes can significantly contribute to protecting the environment, treating contaminated water and reducing the impact of pollution in various areas of our daily life.

Eco-friendly strategies for nanoparticle development mostly use plant extracts. Phyto-mediated syntheses should be encouraged in terms of ecological aspects, simple and large-scale production of nanomaterials. NP-ZnO have been widely developed by plant extracts in recent years. ZnO NPs are a highly versatile material and it is noteworthy that several phytogenic ZnO NPs show similar or improved potentials compared to chemically derived samples.

While alginate-based composites typically exhibit improved physical/mechanical properties over pure alginate gels or spheres, the biocompatibility of alginate coupled with novel properties of encapsulated materials often provide synergistic functionalities of new derivatives. These include the ease of biosorbent separation and regeneration for wastewater treatment, the reduced risk of encapsulating materials such as nanomaterials and the optimized bioprocesses of microbial immobilization technology being lost to the environment.

Future environmental applications of alginate-based composites, which are likely to evolve considerably, require further research into the mechanisms involved in pollutant uptake by different alginate-based composites. Comparative studies can be performed between composites under controlled laboratory conditions. Another research need is to optimize existing composites and design new alginate-based composites. The studies described in this paper were performed at the laboratory level. Extension to real-world applications in an uncontrolled environment requires further testing, as the characteristics and mechanical/thermal stability of ZnO nanoparticles but also Alg-based composites may change.

In attempts to test alginate-based composites in large-scale applications, cost and efficiency are important factors to be evaluated. Because microbial treatment is potentially less harmful to the environment and more cost-effective than chemical or physical treatments of soil or water, encapsulating microorganisms in alginate spheres will be cost-effective. Investigating the effectiveness of the immobilization technology, particularly in the areas of microbial survival, binding and transport, as well as in situ bioremediation of contaminated soil or groundwater will develop the alginate-based technology and make it more competitive for use in pollutant removal applications from the environment.

VII.2. Original contributions

The research activities carried out during this doctoral internship led to the realization of original contributions in the field of environmental engineering and advanced materials, as follows: (i) extensive bibliographic research from the specialized literature, with references from the period of 2010 until now with regarding the possibility of applying some green syntheses in obtaining nanostructured photocatalytic eco-materials applied in the degradation processes of emergent pollutants as well as increasing the performance of photocatalytic processes by integrating these nanostructures in fixed supports in order to reduce the risk of uncontrolled evacuation due to small dimensions, thus identifying elements of originality with scientific value regarding the use of vegetable waste with reducing rollers in the green synthesis of nanoparticles; (ii) development of an integrated green synthesis method using several types of fruit waste (grapefruit peels, pomelo, grapes) as precursors in the synthesis of ZnO NPs; (iii) designing and obtaining sustainable ZnO and ZnO-Alg type eco-materials, this being obtained by incorporating ZnONP into a biodegradable natural polymer obtained from marine brown algae, in order to reduce the risk of loss of ZnO NP type material, after its use in processes of degradation of emergent pollutants; (iv) the selection and testing of some emerging pollutants present today in underground and surface waters, such as clofibric acid CLF, in order to establish the performances of the eco-materials obtained, in photocatalytic processes; (v) developing and applying a complex experimental program to establish the specific optimal parameters involved in photodegradation, kinetic studies and reusability investigations; (vi) validating the performance of the eco-materials through the detailed investigation of the obtained structures and the development of a work plan that included the application of advanced morphological, structural and dimensional characterization techniques, including studies on the surface chemistry of the obtained eco-materials; (vii) establishing possible reaction mechanisms that led to photodegradation

performances using ZnO obtained from various plant extracts and ZnO-Alg, compared to classic ZnO.

VII.3. Future research directions

- the identification and valorization of possible sources of waste that can constitute precursors in the green synthesis of photocatalytic eco-materials in accordance with the principles of the circular bioeconomy and the protection of natural resources;
- simultaneous testing on polluting species present in real waters in order to identify optimal solutions for integrating photocatalytic processes into existing treatment/purification processes;
- putting the proposed idea into practice in an extended environment to demonstrate that the technology works and is ready for widespread implementation.

SELECTIVE BIBLIOGRAPHY

[1]. Bundschuh, M., Filser, J., Lüderwald, S. et al. Nanoparticles in the environment: where do we come from, where do we go to?. Environ Sci Eur 30, 6 (2018).

[2]. Singh, R.; Dutta, S. A review on H2 production through photocatalytic reactions using TiO2/TiO2-assisted catalysts. Fuels 2018, 220, 607–620.

[3]. Surana, D., Gupta, J., Sharma, S., Kumar, S., Ghosh, P., 2022. A review on advances in removal of endocrine disrupting compounds from aquatic matrices: future perspectives on utilization of agri-waste based adsorbents. Sci. Total Environ. 826, 154129.

[4]. Rtimi, S.; Dionysiou, DD; Pillai, SC; Kiwi, J. Advances in catalytic/photocatalytic bacterial inactivation by nano Ag and Cu coated surfaces and medical devices. Appl. Catal. B Environment. 2019, 240, 291–318.

[5]. A. Król, P. Pomastowski, K. Rafińska, V. Railean-Plugaru, B. Buszewski, Zinc oxide nanoparticles: Synthesis, antiseptic activity and toxicity mechanism, Advances in Colloid and Interface Science 249 (2017) 37–52.

[6]. A. Król, P. Pomastowski, K. Rafińska, V. Railean-Plugaru, B. Buszewski, Zinc oxide nanoparticles: Synthesis, antiseptic activity and toxicity mechanism, Advances in Colloid and Interface Science 249 (2017) 37–52.

[7]. JW Rasmussen, E. Martinez, P. Louka, DG Wingett, Zinc oxide nanoparticles for selective destruction of tumor cells and potential for drug delivery applications, Expert Opin. Deliv drug. 7 (2010) 1063–1077.

[8]. Soumeia Zeghoud, Hadia Hemmami, Bachir Ben Seghir, Ilham Ben Amor, Imane Kouadri, Abdelkrim Rebiai, Mohammad Messaoudi, Shakeel Ahmed, Pawel Pohl, Jesus Simal-Gandara, A review on biogenic green synthesis of ZnO nanoparticles by plant biomass and their applications, Materials Today Communications, Volume 33, 2022, 104747.

[9]. AR Prasad, SM Basheer, IR Gupta, K. Elyas, A. Joseph, Investigation on Bovine SerumAlbumin (BSA) binding efficiency and antibacterial activity of ZnO nanoparticles, Mater. Chem. Phys. 240 (2020) 122115.

[10]. T. Bhuyan, K. Mishra, M. Khanuja, R. Prasad, A. Varma, Biosynthesis of zinc oxide nanoparticles from Azadirachta indica for antibacterial and photocatalytic applications, Mater. Sci. Semicond. Process. 32 (2015) 55–61.

[11]. M. Aminuzzaman, LP Ying, WS Goh, A. Watanabe, Green synthesis of zinc oxide nanoparticles using aqueous extract of Garciniamangostana fruit pericarp and their photocatalytic activity, Bull. Mater. Sci. 41 (2018) 0050.

[12]. C. Anupama, A. Kaphle, G. Nagaraju Udayabhanu, Aegle marmelos assisted facile combustion synthesis of multifunctional ZnO nanoparticles: study of their photoluminescence, photo catalytic and antimicrobial activities, J. Mater. Sci. Mater. Electron. 29 (2018) 4238–4249.

[13]. MH Kahsay, A. Tadesse, D. RamaDevi, N. Belachew, K. Basavaiah, Green synthesis of zinc oxide nanostructures and investigation of their photocatalytic and bactericidal applications, RSC Adv. 9 (2019) 36967–36981.

[14]. HY Chai, SM Lam, JC Sin, Green synthesis of magnetic Fe-doped ZnO nanoparticles via Hibiscus rosa-sinensis leaf extracts for boosted photocatalytic, antibacterial and antifungal activities, Mater. Lett. 242 (2019) 103–106.

[15]. L. Chen, I. Batjikh, J. Hurh, Y. Han, Y. Huo, H. Ali, JF Li, EJ Rupa, JC Ahn, R. Mathiyalagan, DC Yang, Green synthesis of zinc oxide nanoparticles from root extract of Scutellaria baicalensis and its photocatalytic degradation activity using methylene blue, Optik 184 (2019) 324–329.

[16]. N. Elavarasan, K. Kokila, G. Inbasekar1, V. Sujatha, Evaluation of photocatalytic activity, antibacterial and cytotoxic effects of green synthesized ZnO nanoparticles by Sechium edule leaf extract, Res. Chem. Intermediate 43 (2017) 3361–3376.

[17]. K. Elumalai, S. Velmurugan, S. Ravi, V. Kathiravan, S. Ashokkumar, Green synthesis of zinc oxide nanoparticles using Moringa oleifera leaf extract and evaluation of its antimicrobial activity, Spectrochim. Acta A Mol. Biomol. spectrosc. 143 (2015) 158–164.

[18]. J. Fowsiya, G. Madhumitha, NA Al-dhabi, M. Valan, Biology photocatalytic degradation of Congo red using Carissa edulis extract capped zinc oxide nanoparticles, J. Photochem. Photobiol. B 162 (2016) 395–401.

[19]. VV Gawade, NL Gavade, HM Shinde, SB Babar, AN Kadam, KM Garadkar, Green synthesis of ZnO nanoparticles by using Calotropis procera leaves for the photodegradation of methyl orange, J. Mater. Sci. Mater. Electron. 28 (2017) 14033–14039.

[20]. OK Hee, EJ Rupa, G. Anandapadmanaban, M. Chokkalingam, JF Li, J. Markus, V. Soshnikova, ZEJ Perez, DC Yang, Cationic and anionic dye degradation activity of Zinc oxide nanoparticles from Hippophae rhamnoides leaves as potential water treatment resource , Optik 181 (2019) 1091–1098.

[21]. Suresh D, Nethravathi PC, Rajanaika H, Nagabhushana H, Sharma SC., Green synthesis of multifunctional zinc oxide (ZnO) nanoparticles using Cassia fistula plant extract and their photodegradative, antioxidant and antibacterial activities, Mater Sci Semicond Process (2015); 31:446–54.
[22]. PlasticsEurope, Plastics -The facts 2019 - An analysis of European plastics production, demand and waste data <https://www.plasticseurope.org/application/files/9715/7129/9584/FINAL_web_version_Plastics_the_ facts2019_14102019.pdf> (2019).
[23]. Testing of Alginate/Chitosan/Glass Bubbles Adsorbent for Copper Removal from Wastewater E. MATEI , AM PREDESCU, M. RAPA, A. TURCANU , C. PREDESCU , R. VIDU , L. FAVIER , CLCOVALIU , D. IGNAT , V. GRIGORE , Plastic MaterialsVolume58, Issue1, Page19-26; 2021
[24]. Mohammadi, A., Daemi, H., & Barikani, M., Fast removal of malachite green dye using novel superparamagnetic sodium alginate-coated Fe3O4 nanoparticles. International Journal of Biological Macromolecules, 69, (2014), 447–455.
[25]. PC Nagajyothi, S. Ju, I. Jun, TVM Sreekanth, K. Joong, H. Mook, Biology antioxidant and anti-inflammatory activities of zinc oxide nanoparticles synthesized using Polygala tenuifolia root extract, J. Photochem. Photobiol. B 146 (2015) 10–17.
[26]. J. Fowsiya, G. Madhumitha, NA Al-dhabi, M. Valan, Biology photocatalytic degradation of Congo red using Carissa edulis extract capped zinc oxide nanoparticles, J. Photochem. Photobiol. B 162 (2016) 395–401.
[27]. European Commission, 2008. Priority Substances Daughter Directive-directive 2008/105/EC of the European Parliament and of the Council of 16 December 2008 on Environmental Quality Standards in the Field of Water Policy.
[28]. Khenniche L., Favier L., Bouzaza A., Fourcade F., Aissani F., Amrane A., Photocatalytic degradation of bezacryl yellow in batch reactors-feasibility of the combination of photocatalysis and a biological treatment, Environmental Technology (2015), 36, 1–10.
[29]. Anand, U., Dey, S., Bontempi, E, et al., Biotechnological methods to remove microplastics: a review (2023), Environmental Chemistry Letters, in press.
[30]. P. Chen, et al., Photocatalytic degradation of clofibric acid by g-C3N4/P25 composites under simulated sunlight irradiation: the significant effects of reactive species, Chemosphere 172 (2017) 193–200.
[31]. Joshua O. Ighaloa, Oluwaseun Jacob Ajalab, Great Umenwekec, Samuel Ogunniyia, Comfort Abidemi Adeyanjua, Chinenye Adaobi Igwegbed, Adewale George Adeniyia, Mitigation of clofibric acid pollution by adsorption: A review of recent developments, Journal of Environmental Chemical Engineering 8 (2020) 104264.
[32]. J. Corcoran, MJ Winter, A. Lange, R. Cumming, SF Owen, CR Tyler, Effects of the lipid regulating drug clofibric acid on PPARα-regulated gene transcript levels in common carp (Cyprinus carpio) at pharmacological and environmental exposure levels, Aquat . Toxicol. 161 (2015) 127–137.
[33]. Kais, Hiba & Yeddou Mezenner, Nacèra & Trari, M. & Madjene, Farid. (2019). Photocatalytic Degradation of Rifampicin: Influencing Parameters and Mechanism. Russian Journal of Physical Chemistry A. 93. 2834-2841.
[34]. GK Jayaprakasha, DV Dandekar, SE Tichy, and BS Patil, "Simultaneous separation and identification of limonoids from citrus using liquid chromatography-collision-induced dissociation mass spectra," Journal of Separation Science, vol. 34, no. 1, (2011) pp. 2–10.
[35]. K. Khosravi-Darani, A. Gomes da Cruz, E. Shamloo, Z. Abdimoghaddam, MR Mozafari, "Green synthesis of metallic nanoparticles using algae and microalgae", Letters in Applied NanoBio, Science 8 (2019) 666–670.
[36] Thongam, DD, Gupta, J. & Sahu, NK Effect of induced defects on the properties of ZnO nanocrystals: surfactant role and spectroscopic analysis. SN Appl. Sci. 1, 1030 (2019). https://doi.org/10.1007/s42452-019-1058-3
[37]. Addi, M.; Elbouzidi, A.; Abid, M.; Tungmunnithum, D.; Elamrani, A.; Hano, C. An Overview of Bioactive Flavonoids from Citrus Fruits. Appl. Sci. 2022, 12, 29.
[38]. Kumar, Brajesh et al. "Green approach for fabrication and applications of zinc oxide nanoparticles." Bioinorganic chemistry and applications vol. 2014 (2014): 523869.
[39]. Enyioma C. Okpara, Omolola E. Fayemi, El-Sayed M. Sherif, Harri Junaedi and Eno E. Ebenso, Green Wastes Mediated Zinc Oxide Nanoparticles: Synthesis, Characterization and Electrochemical Studies, Materials 2020, 13, 4241.
[40]. AM Dugandzic et al., Effect of inorganic ions, photosensitisers and scavengers on the photocatalytic degradation of nicosulfuron, Journal of Photochemistry and Photobiology A: Chemistry 336 (2017) 146–155
[41]. A. Ghosh, A. Nayak, A. Pal, Nano-particle-mediated wastewater treatment: a review, Curr. Polluted. Rep. 3 (2017) 17–30.
[42]. Sarasidis VC, Plakas KV, Patsios SI, Karabelas AJ, Investigation of diclofenac degradation in a continuous photo-catalytic membrane reactor. Influence of operating parameters, Chemical Engineering Journal (2014), 239, 299-311.

[43]. Athanasios Tsiampalis, Zacharias Frontistis, Vassilios Binas, George Kiriakidis and Dionissios Mantzavinos, Degradation of Sulfamethoxazole Using Iron-Doped Titania and Simulated Solar Radiation, Catalysts 2019, 9, 612.
[44]. Rana Sabouni1 & Hassan Gomaa, Photocatalytic degradation of pharmaceutical micro-pollutants using ZnO, Environmental Science and Pollution Research (2019) 26:5372–5380.
[45]. Edris Bazrafshana, Tariq J. Al-Musawib, Marcela Fernandes Silvac, Ayat Hossein Panahid, Mohammad Havangie, Ferdos Kord Mostafapure, Photocatalytic degradation of catechol using ZnO nanoparticles as catalyst: Optimizing the experimental parameters using the Box-Behnken statistical methodology and kinetic studies, Microchemical Journal 147 (2019) 643–653.
[46]. Petala, A.; Noah, A.; Frontistis, Z.; Drivas, C.; Kennou, S.; Mantzavinos, D.; Kondarides, DI Synthesis and characterization of CoOx/BiVO4 photocatalysts for the degradation of propyl paraben. J. Hazard. Mater. 2019,372, 52–60.
[47]. Ashraf Shafaei, Manouchehr Nikazar, Mokhtar Arami, Photocatalytic degradation of terephthalic acid using titania and zinc oxide photocatalysts: Comparative study, Desalination 252 (2010) 8–16.
[48]. Choi, J.; Lee, H.; Choi, Y.; Kim, S.; Lee, S.; Lee, S.; Choi, W.; Lee, J. Heterogeneous photocatalytic treatment of pharmaceutical micropollutants: Effects of wastewater effluent matrix and catalyst modifications. Appl. Catal. B Environment. 2014, 147, 8–16.
[49]. Athanasios Tsiampalis, Zacharias Frontistis, Vassilios Binas, George Kiriakidis and Dionissios Mantzavinos, Degradation of Sulfamethoxazole Using Iron-Doped Titania and Simulated Solar Radiation, Catalysts 2019, 9, 612.
[50]. Bai X, Wang L, Zong R, Lv Y, Sun Y, Zhu Y. Performance enhancement of ZnO photocatalyst via synergic effect of surface oxygen defect and grapheme hybridization. Langmuir. 2013;29(9):3097–105.
[51]. Chen TT, Chang IC, YangMH, Chiu HT, Lee CY. The exceptional photo-catalytic activity of ZnO/RGO composite via metal and oxygen vacancies. Appl Catal B. 2013;142–143:442–9.
[52]. Lee KM, Hamid SBA, Lai CW. Multivariate analysis of photocatalytic-mineralization of eriochrome black T dye using ZnO catalyst and UV irradiation. Mater Sci Semicond Process. 2015; 39:40–8
[53]. Gautam, DP, Rahman, S., Fortuna, A.-M., Borhan, MS, Saini-Eidukat, B., & Bezbaruah, AN, Characterization of zinc oxide nanoparticles (NZNO) alginate beads in reducing gaseous emission from swine manure . Environmental Technology, 38(9), (2017), 1061–1074.
[54]. Majeed Khan, MA; Siwach, R.; Kumar, S.; Alhazaa, AN Role of Fe doping in tuning photocatalytic and photoelectrochemical properties of TiO2 for photodegradation of methylene blue. Eight. Laser Technol. 2019, 118, 170–178.
[55]. Hong, H.-J., Jeong, HS, Kim, B.-G., Hong, J., Park, I.-S., Ryu, T., Ryu, J., Highly stable and magnetically separable alginate/ Fe3O4 composite for the removal of strontium (Sr) from seawater. Chemosphere, 165, (2016), 231–238.
[56]. Elwakeel, KZ, Daher, A., Abd El-Fatah, A., Abd El Monem, H., & Khalil, MM, Biosorption of lanthanum from aqueous solutions using magnetic alginate beads. Journal of Dispersion Science and Technology, 38(1), (2017), 145–151.